DEPARTMENT OF TRANSPORTATION

Comparison of the Performance of Fiber Reinforced Plastic Dowel Bars to Epoxy-Coated and Stainless-Steel Dowel Bars

Annika Christiansen, Principal Investigator
Office of Materials and Road Research
Minnesota Department of Transportation

MAY 2023

Research Project
Final Report 2022-25

MnROAD
SAFER, SMARTER, SUSTAINABLE PAVEMENTS THROUGH INNOVATIVE RESEARCH

To request this document in an alternative format, such as braille or large print, call 651-366-4718 or 1-800-657-3774 (Greater Minnesota) or email your request to ADArequest.dot@state.mn.us. Please request at least one week in advance.

Technical Report Documentation Page

1. Report No.	2.	3. Recipients Accession No.	
MN 2022-25			
4. Title and Subtitle Comparison of the Performance of Fiber Reinforced Plastic Dowel Bars to Epoxy-Coated and Stainless-Steel Dowel Bars		5. Report Date May 2023 6.	
7. Author(s) Sarah Ziemann, Annika Christiansen & Bernard Izevbekhai		8. Performing Organization Report No.	
9. Performing Organization Name and Address Minnesota Department of Transportation Office of Materials 1400 Gervais Avenue Maplewood, Minnesota 55109		10. Project/Task/Work Unit No. 11. Contract (C) or Grant (G) No.	
12. Sponsoring Organization Name and Address Minnesota Department of Transportation Office of Research & Innovation 395 John Ireland Boulevard, MS 330 St. Paul, Minnesota 55155-1899		13. Type of Report and Period Covered Final Report 14. Sponsoring Agency Code	
15. Supplementary Notes http://mdl.mndot.gov/			

16. Abstract (Limit: 250 words)

The introduction of fiber reinforced plastic (FRP) dowels as possible alternatives to the epoxy-coated and stainless-steel dowels, was contemporaneous with a paucity of knowledge of their long-term performance. Although various isolated efforts had examined them on a short-term basis and produced some qualitative results or long-term predictive models, actual long-term performance in service was still unknown and unanalyzed.

An experiment at the MnROAD Research facility placed FRP dowels in 2000 in some of the jointed plain concrete pavement (JPCP) panels of test Cell 52 and used epoxy-coated dowels in the remaining panels of this cell. The contiguity of this test cell with Cell 53, a JPCP high-performance concrete cell built in 2008 with stainless steel dowels, and Cell 54, a taconite JPCP cell with epoxy-coated dowels in built in 2004, facilitated a comparative analysis of performance of the 3 dowel types particularly in load transfer efficiency (LTE) and ride quality. The difference in the inception of the cells constrained a performance over time and encouraged a time-series autoregressive integrated moving average (ARIMA) analysis. Projections to 30 years showed that LTE and ride quality of FRP dowels were no different from those of the epoxy-coated dowels and the stainless-steel dowels although Cell 53 was designed and built with thicker concrete (12-in. thick) compared to 7.5-in in cells 52 and 54.

17. Document Analysis/Descriptors	18. Availability Statement		
Load transfer, Dowels, Falling weight deflectometers, Roughness, Fiber reinforced plastics	No restrictions. Document available from: National Technical Information Services, Alexandria, Virginia 22312		
19. Security Class (this report) Unclassified	20. Security Class (this page) Unclassified	21. No. of Pages 47	22. Price

COMPARISON OF THE PERFORMANCE OF FIBER REINFORCED PLASTIC DOWEL BARS TO EPOXY-COATED AND STAINLESS-STEEL DOWEL BARS

FINAL REPORT

Prepared by:

Sarah Ziemann
Mechanical Engineering & Materials Science
Student Worker Paraprofessional Snr.
Office of Materials and Road Research, Minnesota Department of Transportation

Annika Christiansen
Mathematics and Statistics
Student Worker Paraprofessional Snr.
Office of Materials and Road Research, Minnesota Department of Transportation

MAY 2023

Published by:

Minnesota Department of Transportation
Office of Research & Innovation
395 John Ireland Boulevard, MS 330
St. Paul, Minnesota 55155-1899

ACKNOWLEDGMENTS

We acknowledge Dr. Bernard Igbafen Izevbekhai, MnDOT research operations engineer, who birthed the idea of conducting this study, guided the authors in their data analysis and research, and reviewed the report various times. We also benefited immensely from the feedback of Benjamin Worel, MnROAD operations engineer, and Thomas Burnham, senior road research engineer, at the Office of Materials and Road Research. Authors are also indebted to Jacob Calvert, MnROAD monitoring engineer. The study would not have been possible without continual support from Jeffrey Brunner, road research director, and Glenn Engstrom, office director, at MnDOT's Office of Materials and Road Research.

TABLE OF CONTENTS

LIST OF FIGURES

LIST OF TABLES

EXECUTIVE SUMMARY

Falling weight deflectometer (FWD) testing has been commonly used on various pavement surfaces to better understand the response of pavement to different dynamic loads. Routine FWD testing has been performed on cells 52, 53, and 54 of Minnesota's Road Research Facility since their construction in 2000, 2008, and 2004, respectively. Cell 52 is a Portland cement concrete, which consists of fiber-reinforced plastic (FRP) dowel bars and epoxy-coated steel dowels, Cell 53 is a 60-year design of high-performance concrete with stainless-steel dowel bars, and Cell 54 is a Mesabi-select aggregate in Portland cement concrete with epoxy-coated steel bars. FWD testing can help analyze the effectiveness of the dowel bars in each of these cells. Although the ability of non-steel dowels in comparison to steel dowels has been questioned, the cross-sections of all the dowels are the same. Thus, this research helps to better understand the actual load transfer efficiencies (LTEs) of the dowels.

To understand the load transfer efficiencies of the dowels, falling weight deflectometer tests were performed before the joint and after the joint. These tests provided information on the deflection at each point, while taking a ratio of the deflections resulted in load transfer efficiency. The data collected on cells 52, 53, and 54 were clustered by the stresses used in the loading and by joint within each cell. Then, curve fitting via interpolation was used to ensure that spring and fall of each year had data. Time-series analysis was used to understand the overall trends of the LTE for each cell and make a prediction 15-years and 30-years post-construction.

Time series analysis involved using Autoregressive Moving Average Integrated models and Excel's Solver function. Using Akaike information criterion, Bayesian information criterion, and the smallest sum of squared error terms in Excel helped to determine the best model, where the model coefficients allowed the data to converge and provided an accurate prediction of future load transfer efficiencies.

The International Roughness Index (IRI) was also used to measure the ride quality of the pavement and the performance of the concrete. Measurements for IRI occurred approximately three times a year at MnROAD to observe ride performance trends. The IRI values for cells 52, 53, and 54 helped to better understand pavement performance as a whole.

The Cell 52 FRP dowel bars performed relatively similarly to the other dowel bars, yet it seems that the overall data indicated that the epoxy-coated dowel bars had a higher LTE than the FRP dowel bars in Cell 52. All the LTEs of these FRP dowel bars were near 0.8. The stainless-steel dowel bars found in the high-performance concrete of Cell 53 performed similarly to the FRP dowels in Cell 52. The 30-year prediction seemed to indicate that Cell 53 had a slightly higher LTE prediction for 30 years (0.89 for the lane loaded consistently and 0.86 for the control lane, which is never subjected to loading) as compared to the prediction for Cell 52 of the FRP dowel bars (0.84 for the loaded lane and 0.87 for the unloaded lane). The traditional epoxy-coated dowel bars in Cell 54 had the highest predictions for 15- and 30-year performance trends in LTE. Both the 15- and 30-year predictions indicated an LTE of 0.94 and 0.97 for the loaded lane and unloaded lane, respectively. It was difficult to make overarching conclusions about the effectiveness of the dowels due to challenges in time-series modeling, differences in timing and

construction of the concretes, as well as contrasts between the concrete used to construct the cells themselves.

The IRI data revealed that Cell 53, the 60-year design of high-performance concrete, had the highest IRI and therefore the smoothest ride. All the cells had similar IRI values, which levels the advantages of certain dowel bars. Other various tests to analyze ease of construction, length of effective performance, and availability and sustainability of materials should be performed to gain more understanding about fiber-reinforced plastic dowels.

According to the models developed in this paper, the FRP dowels do provide an effective response to different dynamic loads for PCC concrete pavements throughout a 30-year lifetime. The FRP dowels indicate they will continue to sustain an LTE of 80% into 30 years of performance. Future use of these dowel bars should be dependent on the time and intensity of construction, available materials, and other external factors.

CHAPTER 1: INTRODUCTION

1.1 BACKGROUND

The Minnesota Road Research Facility, commonly known as MnROAD, is a full-scale outdoor pavement testing facility located in Monticello (about 40 miles northwest of downtown St. Paul, Minnesota), owned and operated by the Minnesota Department of Transportation (MnDOT). The test track was constructed in 1993 to validate prevailing pavement designs and improve new and efficient designs and materials. The original test sections were created between 1991 and 1994, and the tracks were open to traffic loading on July 15, 1994. MnROAD consists of three test tracks: the Mainline, a 3.5-mile 2-lane westbound section that receives live traffic diverted off the adjacent Interstate 94, the original westbound (OWB) lanes, which carry traffic a few days each month when traffic is diverted from the Mainline, and the Low Volume Road (LVR), a 2.5-mile loop loaded with a 5-axle, 80-kilo-pound semi-trailer that makes 80 laps per day 5 days a week on the inside lane. The outside lane of the LVR is subject to environmental loading only, which acts as a control in comparison to the inside lane. The second phase of MnROAD, from 2008-2016, focused on building new test cells and performing research in materials, design, and pavement surface characteristics studies. The facility is currently beginning its fourth phase of construction and research, which will focus on sustainability and resiliency. MnROAD continues to provide data and research findings to the public at no charge. Currently, MnROAD consists of more than 80 test sections. The LVR consists of around 40 test sections, and the OWB consists of more than 40 test sections. Full details on the history and current test sections of MnROAD can be found on the MnROAD website (1).

This research will focus on cells 52, 53, and 54 located in the LVR of MnROAD. These are part of MnROAD's phase one and two construction events, built in 2000, 2008, and 2004, respectively.

Cell 52, constructed in June and July of 2000, consists of a 7.5-in, top layer of Portland cement concrete. Joints are spaced 15-ft. apart in the cell, and 1-in. diameter and 18-in. long fiber-reinforced plastic (FRP) dowel bars are used in the 13-ft to 14-ft wide section with an Astro-turf finish. Of the 18 panels in the test section, panels 4 to 9 had the FRP dowel bars, and the rest of the panels had conventional epoxy-coated steel dowel bars (2). Below the concrete is a 5-in layer of Class 4 aggregate base and then a deep layer of clay. This can be seen in Figure 1 (3).

Cell 53, also in Figure 1, is composed of the 60-year design of high-performance concrete. It was constructed in October 2008 and contains 1.5-in. diameter and 15-in. long stainless-steel dowel bars. The PCC is 12-ft. deep and 12-ft. wide, and it has a transverse bottom finish. A 5-in. Class 5 aggregate base is placed below the PCC, followed by a 36-in. select granular base (4).

Cell 54, constructed in October 2004, is composed of the Mesabi-select aggregate in PCC. Mesabi-select is a material formed from deposits of iron ore and has been shown to be a useful aggregate in concrete. It is 7.5-in. deep, 15-ft. long, and 12-ft. wide, and it has an astro-turf finish. This cell consists of epoxy-

coated 1-in. diameter and 15-in. long dowel bars, which are standard in concrete pavement use. Below the PCC is a 12-in Class 6 aggregate base (5).

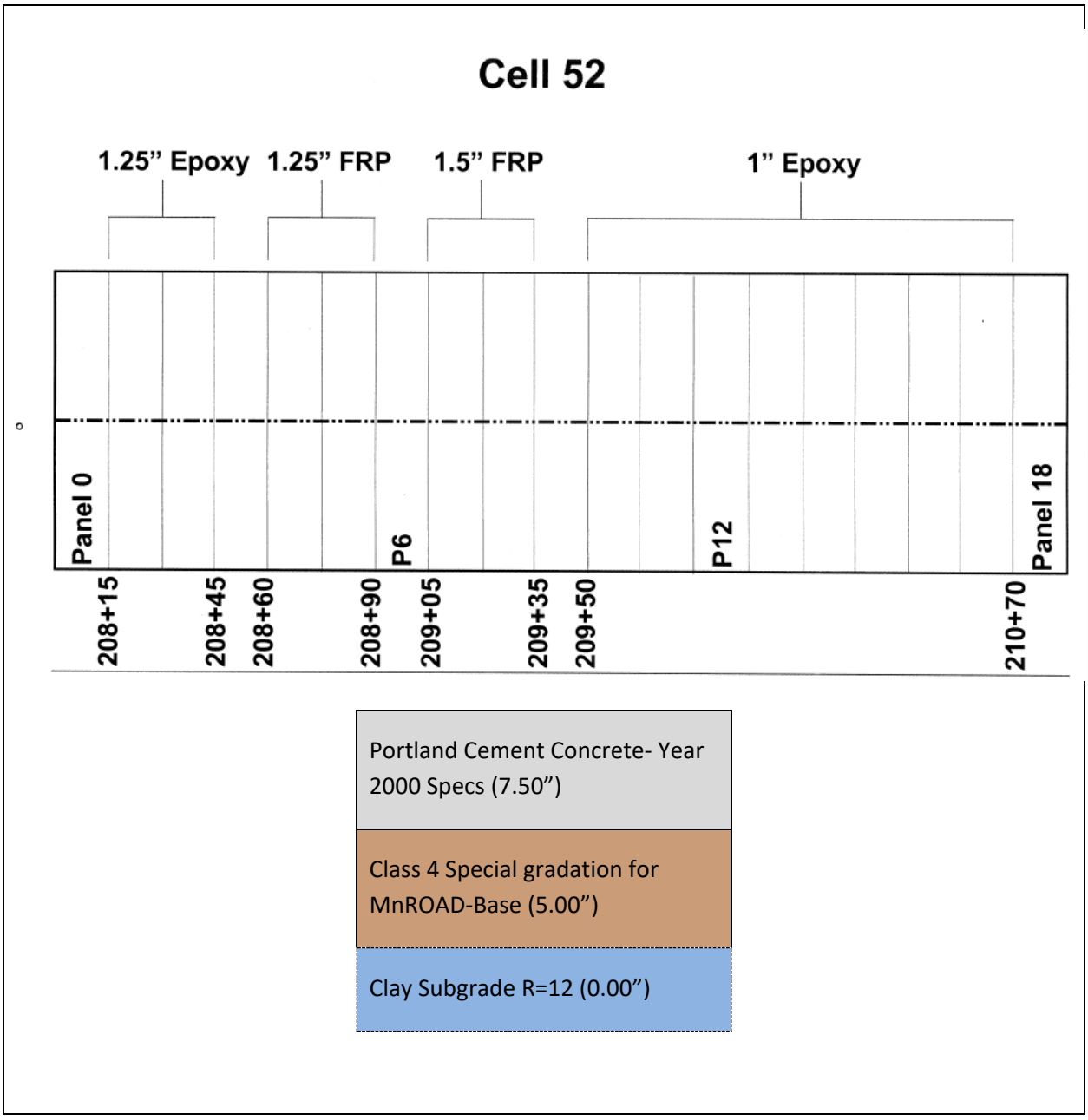

Figure 1.1: Layer Structure Design and Dowel Layout for Cell 52 at MnROAD from Construction Plans (2).

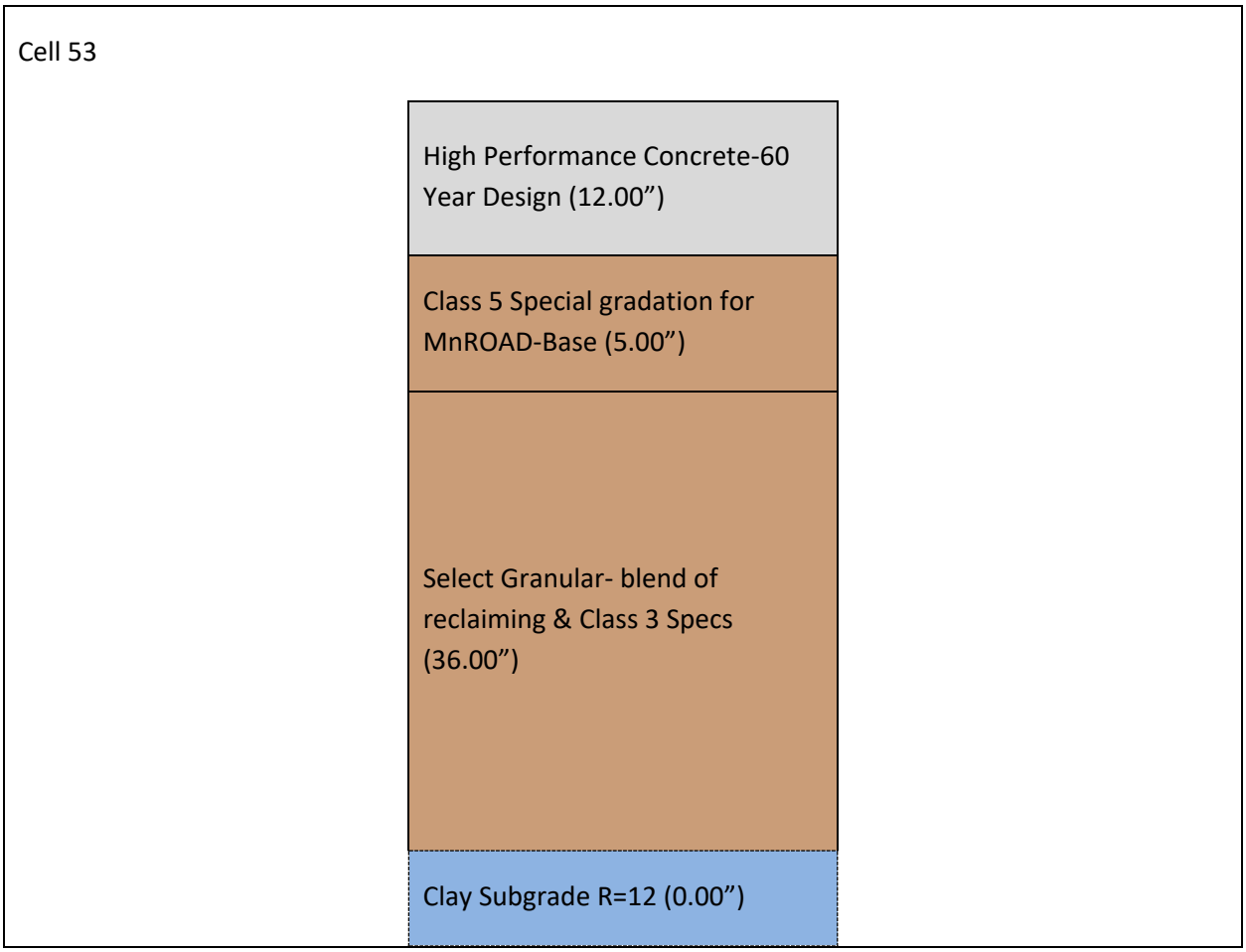

Figure 1.2: Layer Structure Design for Cell 53 at MnROAD.

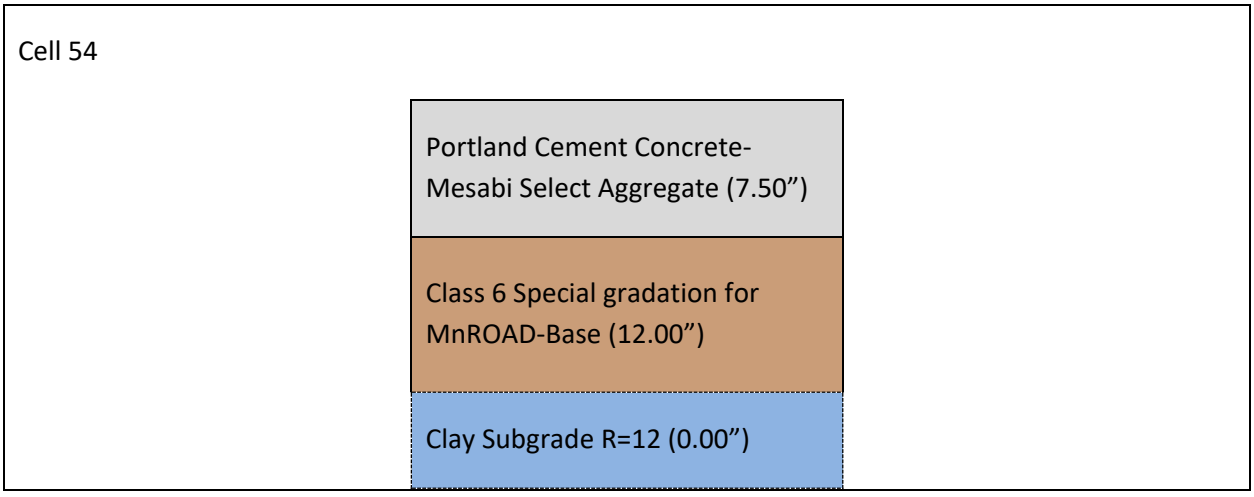

Figure 1.3: Layer Structure Design for Cell 54 at MnROAD.

1.2 OBJECTIVE

This research recognizes the potentially sustainable advantages of using FRP in lieu of steel dowels. Generally, practitioners question the ability for innovative non-steel dowels to withstand the bearing forces of dynamic loads. However, the polar moment of inertia is similar when the cross sections are similar. The differences in responses are thus examined by the actual load transfer efficiencies of these dowels in their test sections. This paper examines the response of the fiber reinforced plastic dowels in cell 52 to dynamic loads. It further compares the implied performance to those of the stainless-steel dowels of cell 53 and the conventional epoxy-coated dowels of cell 52 and cell 54 (6).

CHAPTER 2: METHODS

2.1 FALLING WEIGHT DEFLECTOMETER

Since 1994, MnROAD has been using the Dynatest Model 8000 Falling Weight Deflectometer (FWD) to measure the response of pavement layers to different dynamic loads. The FWD, seen in Figure 2.1, is composed of a loading plate, a weight package, geophone sensors, and data acquisition equipment. The weight package is lifted hydraulically and dropped, providing a dynamic load to the pavement. Geophone sensors capture the resulting deflection basin, which can be used to evaluate the modulus of underlying layers and the structural capacity of the system.

Figure 2.1: Dynatest Model 8000 Falling Weight Deflectometer (FWD)

Routine testing has been performed on cell 52, cell 53, and cell 54 since their constructions in 2000, 2008, and 2004, respectively. Prior to 2008, deflections were collected for 3 drops at each load level of 6000, 9000, and 12000 lbs; post-2008, deflections were collected for 1 drop at each load level of 6000, 9000, and 12000 lbs. On cells 52, 53, and 54, tests were performed in late spring and fall. FWD is performed at various locations in each test slab at the center, edge, corner, before the joint and after the joint. This analysis focuses on the deflections before and after the joint, which help to evaluate the load transfer efficiency of the dowels in the joints.

To test for load transfer efficiency, the FWD trailer is placed so that the joint is between sensors 1 and 3 or 1 and 10 as shown in the FWD trailer setup in Figure 2.2. The load is applied at Sensor 1, and the deflection is measured on the leave slab and the approach slab. The load transfer efficiency can then be calculated through a ratio of these deflections, as in Figure 2.2 (7).

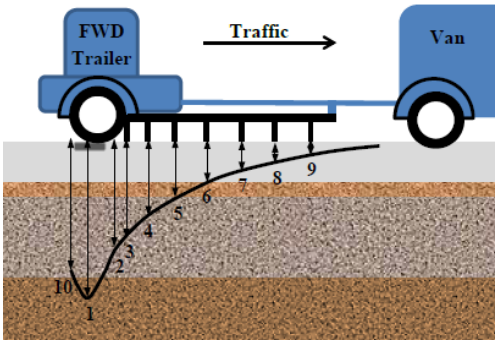

FWD Trailer Setup for LTE and Layer Moduli Analysis

Approach Pavement, Joint Before

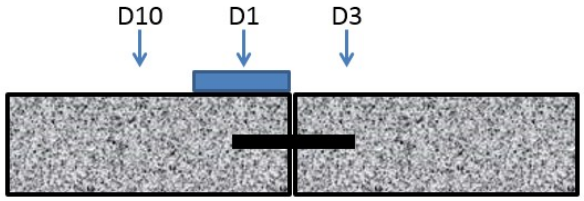

$$LTE = \frac{D3}{D1} * 100\%$$

Leave Pavement, Joint After

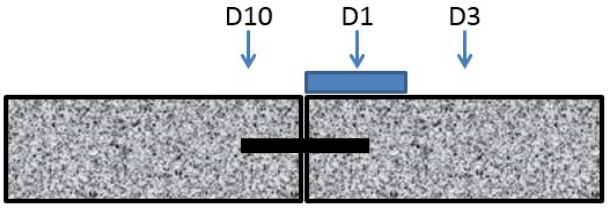

$$LTE = \frac{D10}{D1} * 100\%$$

Figure 2.2: FWD Sensor Setup and Equations

2.2 DATA ORGANIZATION STRATEGY

To understand the modeling and tests that were done on the data, the Falling-Weight Deflectometer data from Cells 52, 53, and 54 from the years 2000-2020 was sorted into categories by load applied. The data was clustered into 365 ± 25 kPA, 550 ± 25 kPA, and 730 ± 25 kPA and sorted by Joint After vs. Joint Before. The data was grouped by joint within each cell, as described in the construction reports. Next, Load Transfer Efficiency (LTE) was calculated for each category and averaged. Then, curve-fitting via interpolation was used to ensure that spring and fall of each year had data. Time-series analysis was used to understand the overall trends of the LTE for each cell and make a prediction 15 and 30 years since construction.

2.3 ANALYTICAL PROCESS

In general, time series data has the form where each data point is indexed in time order, meaning it is a discrete sequence that is taken at successive equally spaced points in time. The FWD data fits a time series model well because, in theory, tests are done at pre-determined times so the "gap" or "interval" between the data points is the same every time. Of the many time series models, the Autoregressive models (AR) and Moving Average models (MA) are the two main models which can be combined to create integrated models, such as the Autoregressive Moving Average Integrated models (ARIMA), used in this analysis (8,9). As in (10), Excel's Solver function was used to determine the coefficients in, for example, **Equation 1** which minimized the sum of square error:

$$Y_t = \phi Y_{t-1} + \varepsilon_t \qquad (1)$$

where $|\phi| < 1$, ε_t is a Normal (white noise) error term.

ARIMA models are dependent on three parameters (p, q, and d) where p is the number of AR terms in the model, d is the number of non-seasonal differences used, and q is the number of lagged forecast errors in the model equation. Multiple ARIMA(p,d,q) models were predicted to fit the data well, and of those tested, the ARIMA(2,1,0) and AR(2) models fit the measured data the best. Understanding which model to choose is difficult, though tools like AIC (Akaike Information Criterion) and BIC (Bayesian Information Criterion) can help decide between two models. In this analysis, multiple models were developed and chosen based on AIC and BIC values, as explained in (11). This time series analysis was implemented in Excel using the Levenberg-Marquardt algorithm for nonlinear least squares curve fitting problems (12). Also considered was the fact that the model coefficients should allow the data to converge instead of having a model which is continuously increasing, as it is not realistic to obtain an LTE which is increasing or predicted to be above 1. That is, **Equation 1** becomes

$$\widehat{Y_t} = c + \theta * \varepsilon_t + \phi_1 Y_{t-1} + \phi_2 Y_{t-2} \qquad (2)$$

or

$$\widehat{Y_t} = \phi_1 Y_{t-1} + \phi_2 Y_{t-2} + c \qquad (3)$$

Where,

$$\widehat{Y_t} = predicted\ LTE\ at\ time\ interval\ t$$

$$Y_t = measured\ LTE\ at\ time\ interval\ t$$

$$\varepsilon_t = difference\ in\ measured\ LTE$$

$$c = constant\ value$$

$$\theta = moving\ average\ (MA)\ coefficient$$

$$\phi_j = j - th\ autoregressive\ (AR)\ coefficient$$

The derived equations are used to make short-term predictions about LTE in the following way:

Table 2.1: Excel implementation of time series model development

Test No	Date	Y(t): Measured	Moving Avg (	Y(t) - Y(t-1)	Y(t-1)-Y(t-2)	Y(t-2)-Y(t-3)	Y(t): Predicted	Error^2
1	SPRING 2008	0.902530527	0.902530527					
2	FALL 2008	0.931017678	0.916774102	0.0284872				
3	SPRING 2009	0.920548444	0.918032216	-0.010469	0.02848715			
4	FALL 2009	0.934315373	0.922103005	0.0137669	-0.0104692	0.02848715	0.937995177	1.3541E-05
5	SPRING 2010	0.920747988	0.921832002	-0.013567	0.01376693	-0.0104692	0.932832205	0.000146028
6	FALL 2010	0.883978965	0.915523162	-0.036769	-0.0135674	0.01376693	0.939288439	0.003059138
7	SPRING 2011	0.895153007	0.91261314	0.011174	-0.036769	-0.0135674	0.916290828	0.000446807
8	FALL 2011	0.931419373	0.914963919	0.0362664	0.01117404	-0.036769	0.893644101	0.001426971
9	SPRING 2012	0.9176	0.915256817	-0.013819	0.03626637	0.01117404	0.91625418	1.81123E-06
10	FALL 2012	0.978859781	0.921617113	0.0612598	-0.0138194	0.03626637	0.937824567	0.001683889
11	SPRING 2013	0.9194	0.921415558	-0.05946	0.06125978	-0.0138194	0.945195089	0.000665387
12	FALL 2013	0.990512334	0.927173622	0.0711123	-0.0594598	0.06125978	0.972016587	0.000342093
13	SPRING 2014	0.966500407	0.93019876	-0.024012	0.07111233	-0.0594598	0.947145948	0.000374595
							SUM	0.00816026

2.4 INTERNATIONAL ROUGHNESS INDEX

While evaluating LTE is intended for efficacy of dowel types, the overall ride quality of the pavement is an indispensable performance indicator. International roughness index (IRI) is the average rectified value (ARV) of the slope of the power spectrum density. It is a measure of roughness of the pavement and is measured with a wide range of equipment including a high-speed van and a lightweight profiler as used at MnROAD (13). Measurements are typically conducted on all MnROAD cells approximately three times a year to observe ride performance trends. The ride performance of Cells 52, 53, and 54 were compared in this research.

CHAPTER 3: RESULTS

First, the LTE data was organized by stress level of FWD drop, lane, and test position (before versus after joint) and plotted over time to obtain a general understanding of the trends (see **Figure 3.1-3.4**).

Cell 52: FRP dowel bars

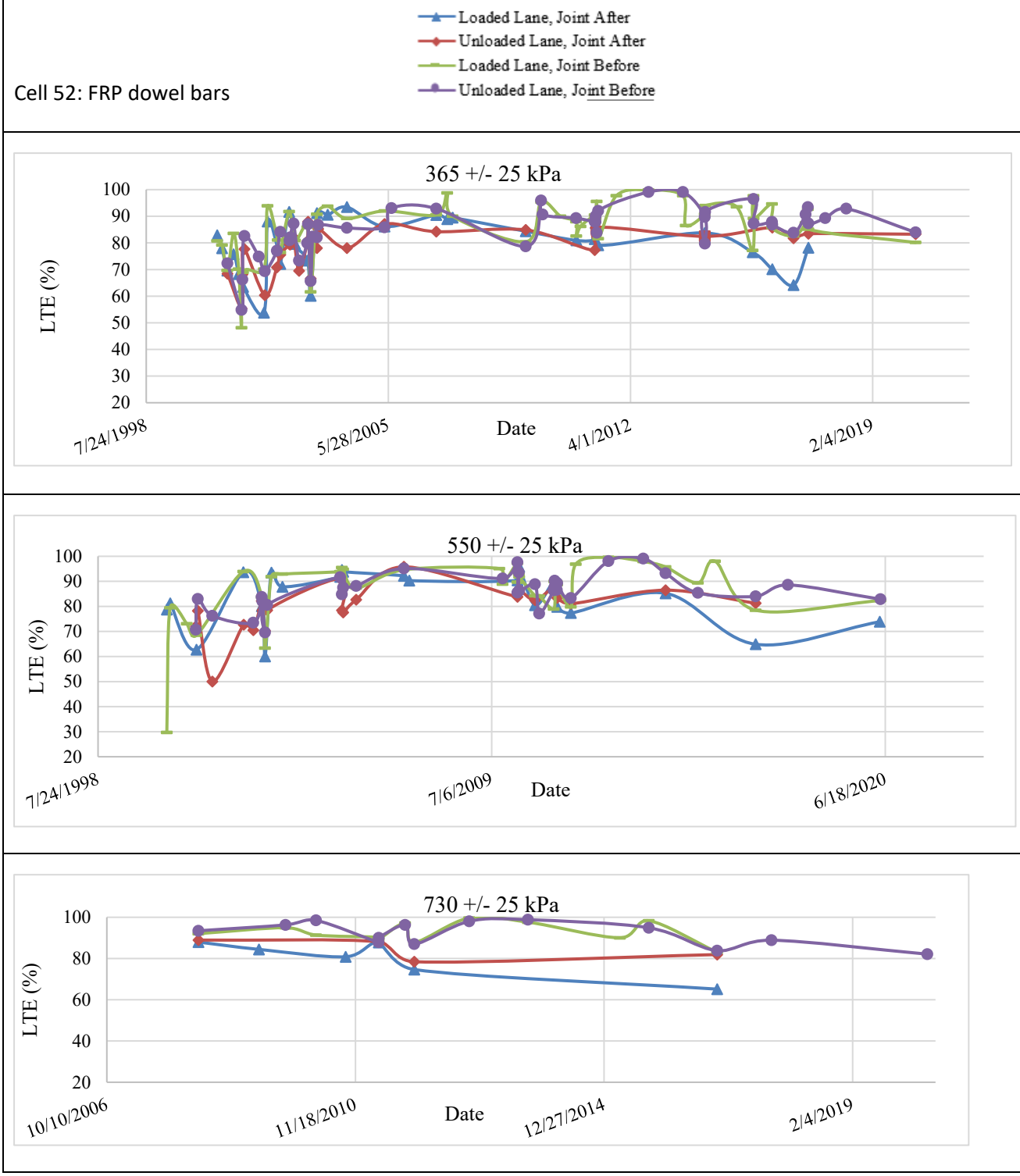

Figure 3.1: Cell 52 FRP dowel bars LTE by stress level (365, 550, and 730 kPa)

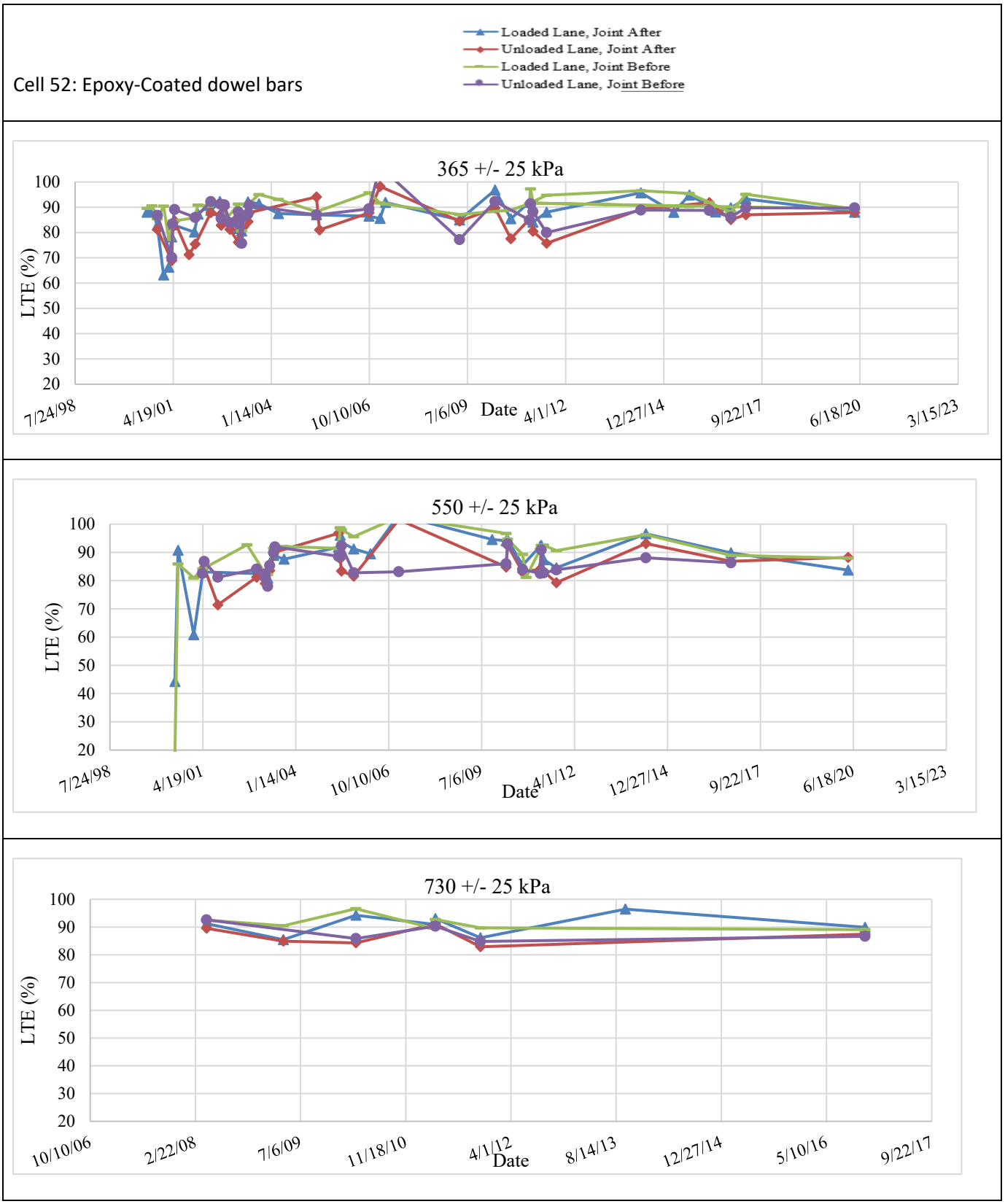

Figure 3.2: Cell 52 epoxy-coated dowel bars LTE by stress level (365, 550, and 730 kPa)

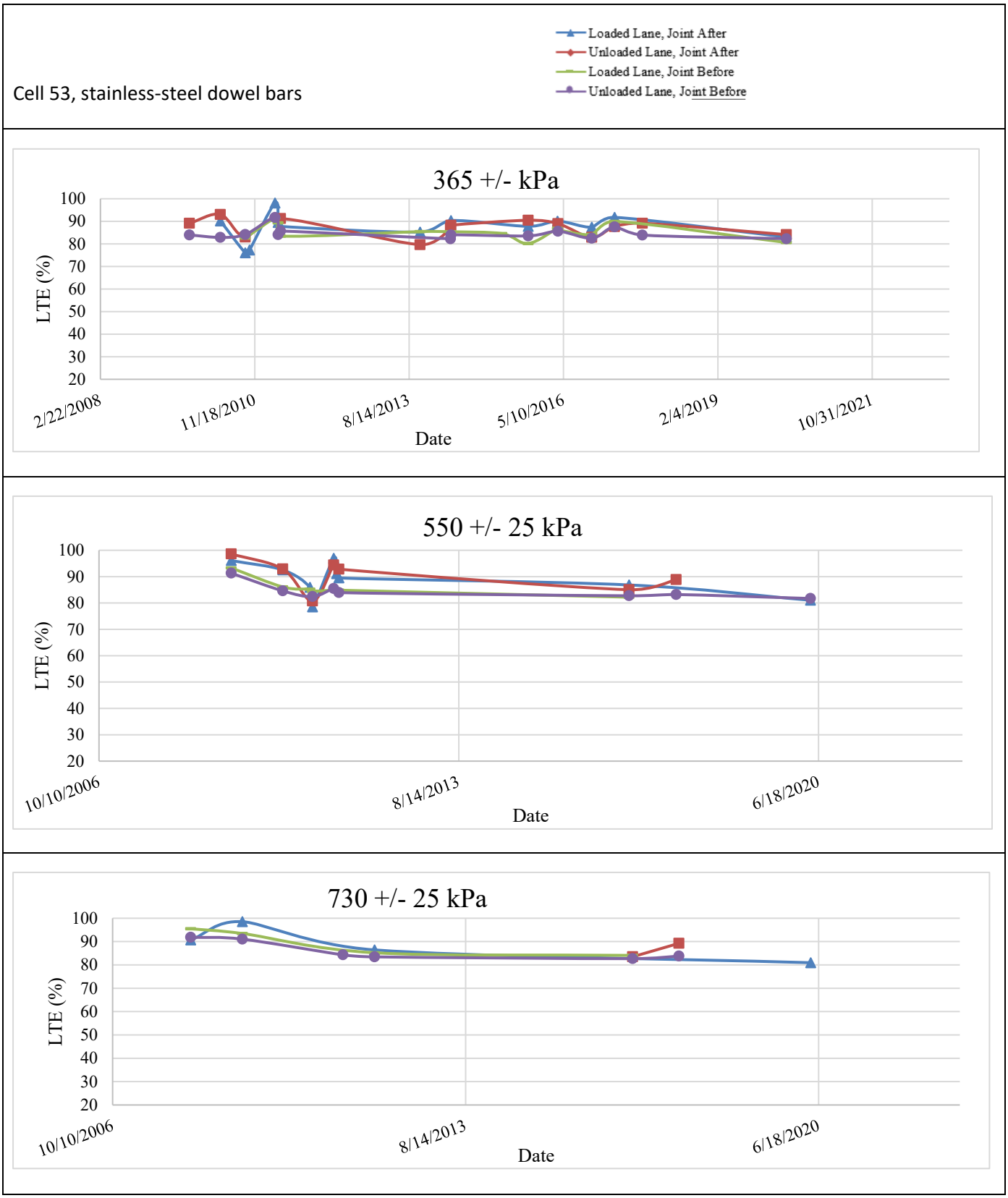

Figure 3.3: Cell 53 LTE by stress level (365, 550, and 730 kPa)

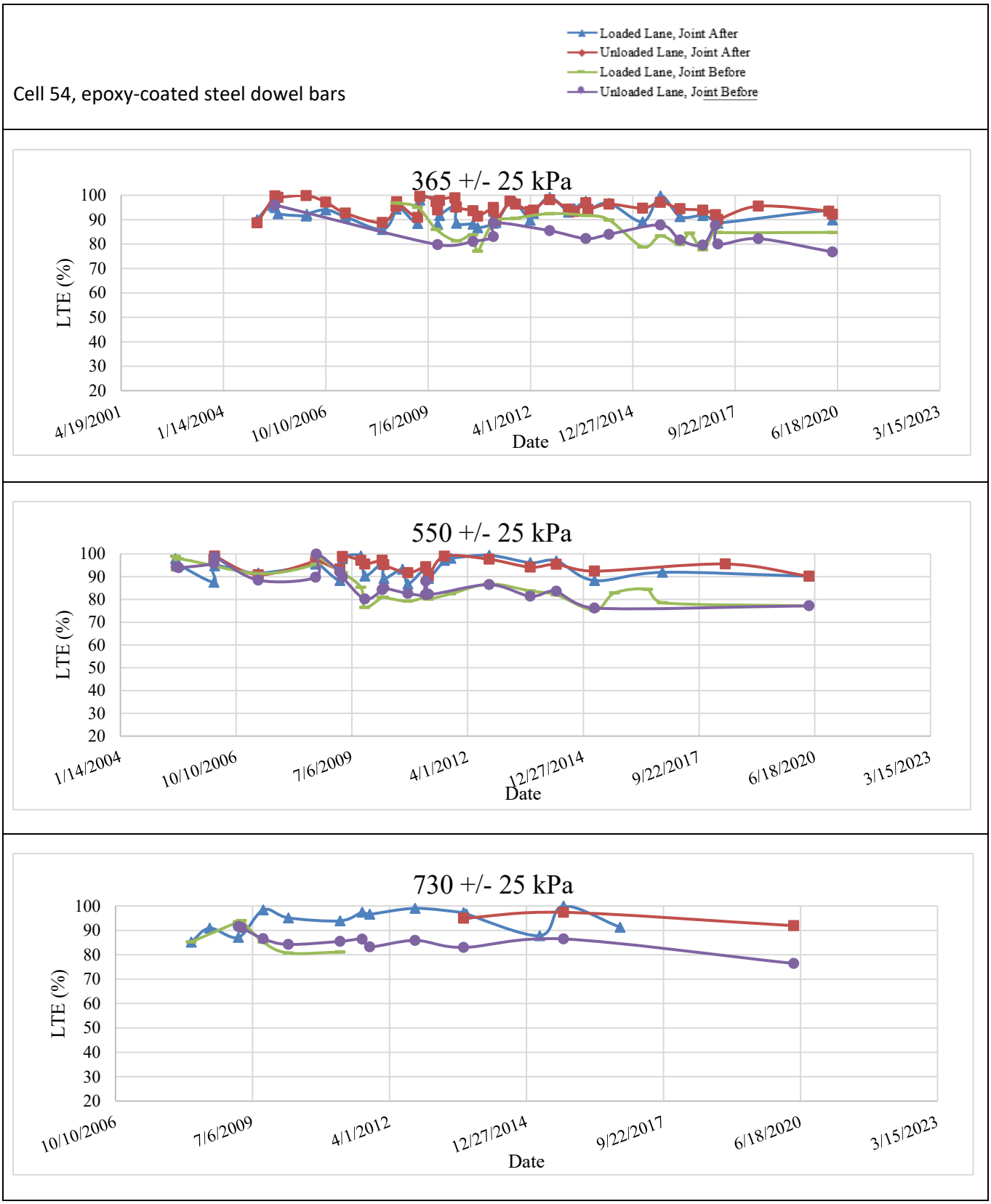

Figure 3.4: Cell 54 LTE by stress level (365, 550, and 730 KPa)

Then, the LTE data was organized by joint, lane, and test position (before versus after joint) and plotted over time to obtain a general understanding of the trends.

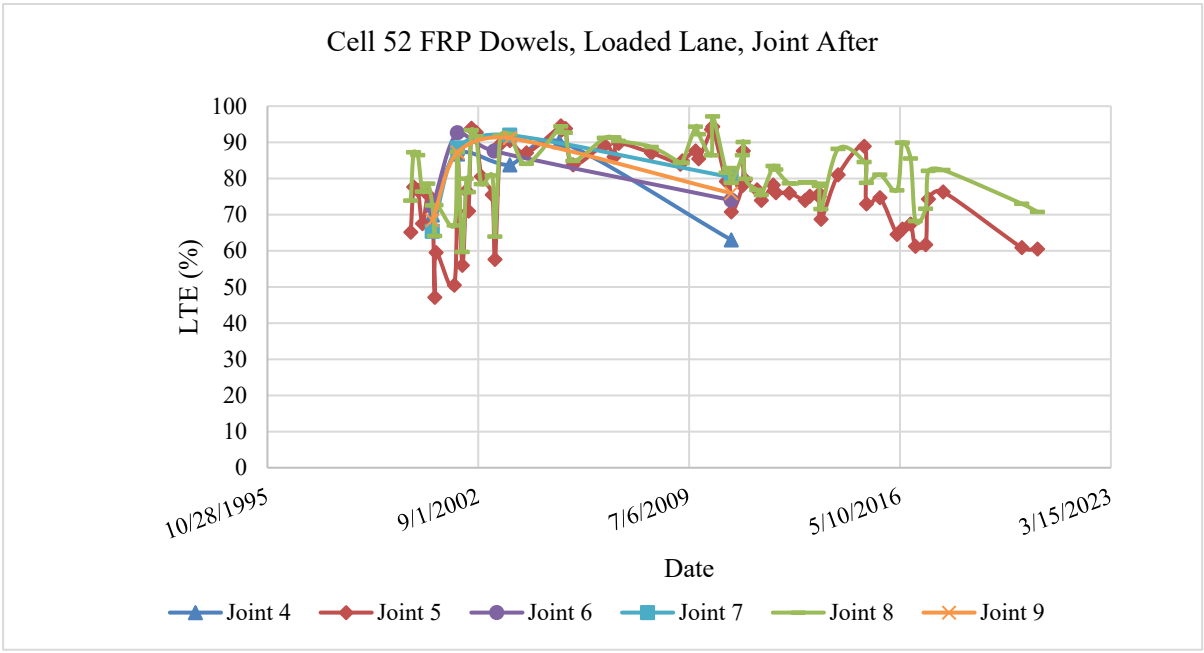

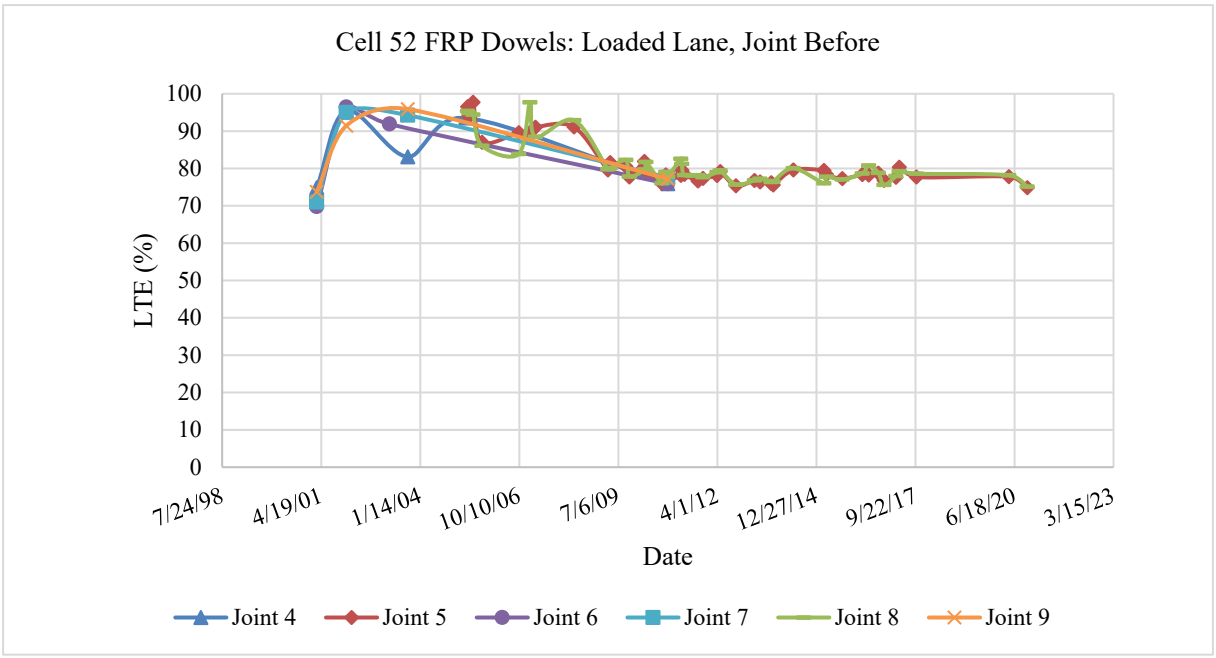

(a)

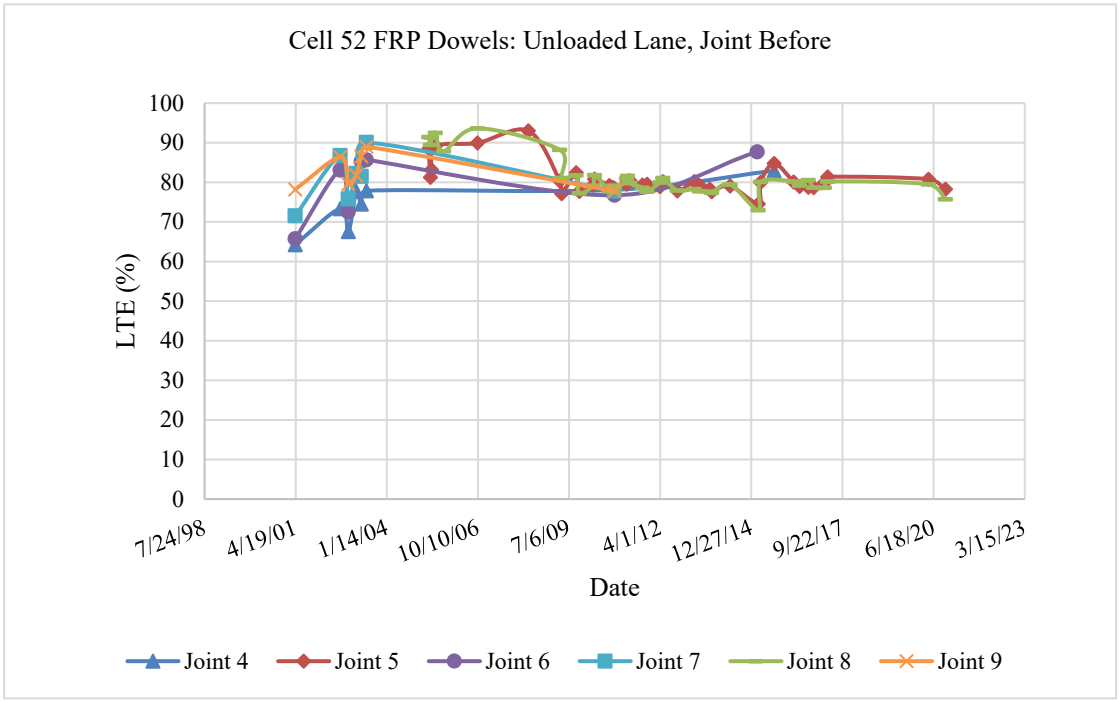

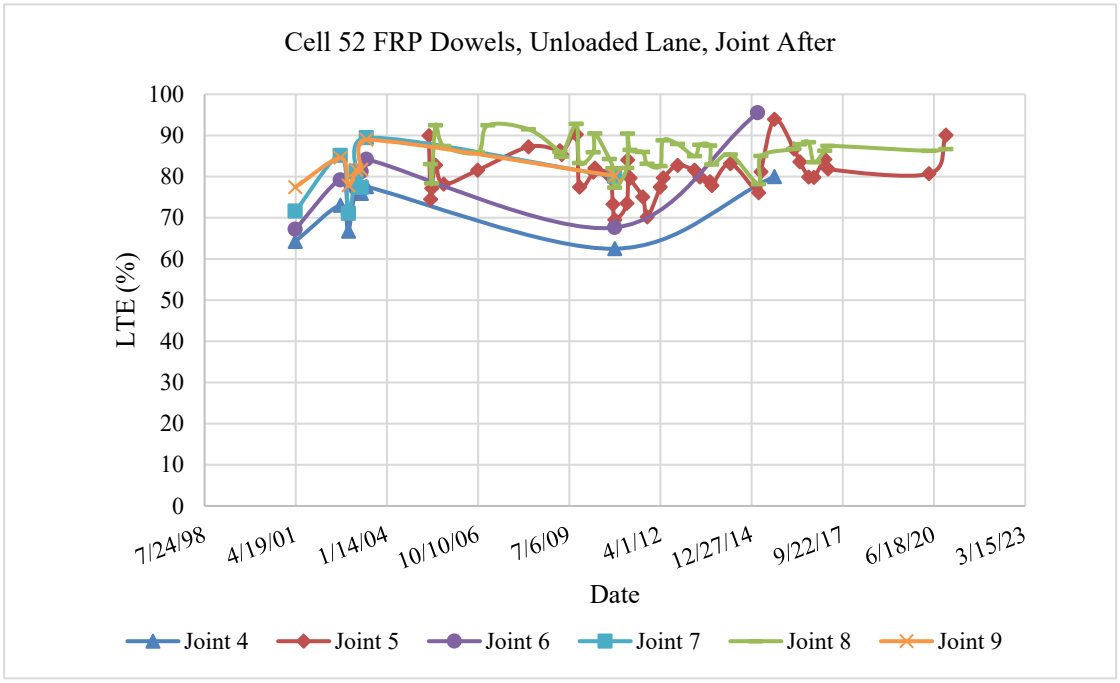

(b)

Figure 3.5 a + b: Cell 52 (FRP dowels) loaded lane LTE by joint


JOINT 0
JOINT 1
JOINT 2
JOINT 3
JOINT 10
JOINT 11
JOINT 12
JOINT 13
JOINT 14
JOINT 15
CELL 52 EPOXY-COATED DOWELS: JOINT AFTER, LOADED LANE
LTE (%)
120
100
80
60
40
20
0
7/24/1998
4/19/2001
1/14/2004
10/10/2006
7/6/2009
4/1/2012
12/27/2014
9/22/2017
6/18/2020
3/15/2023
Date
CELL 52 EPOXY-COATED DOWELS: JOINT BEFORE, LOADED LANE
LTE (%)
120
100
80
60
40
20
0
7/24/1998
4/19/2001
1/14/2004
10/10/2006
7/6/2009
4/1/2012
12/27/2014
9/22/2017
6/18/2020
3/15/2023
Date

(a)

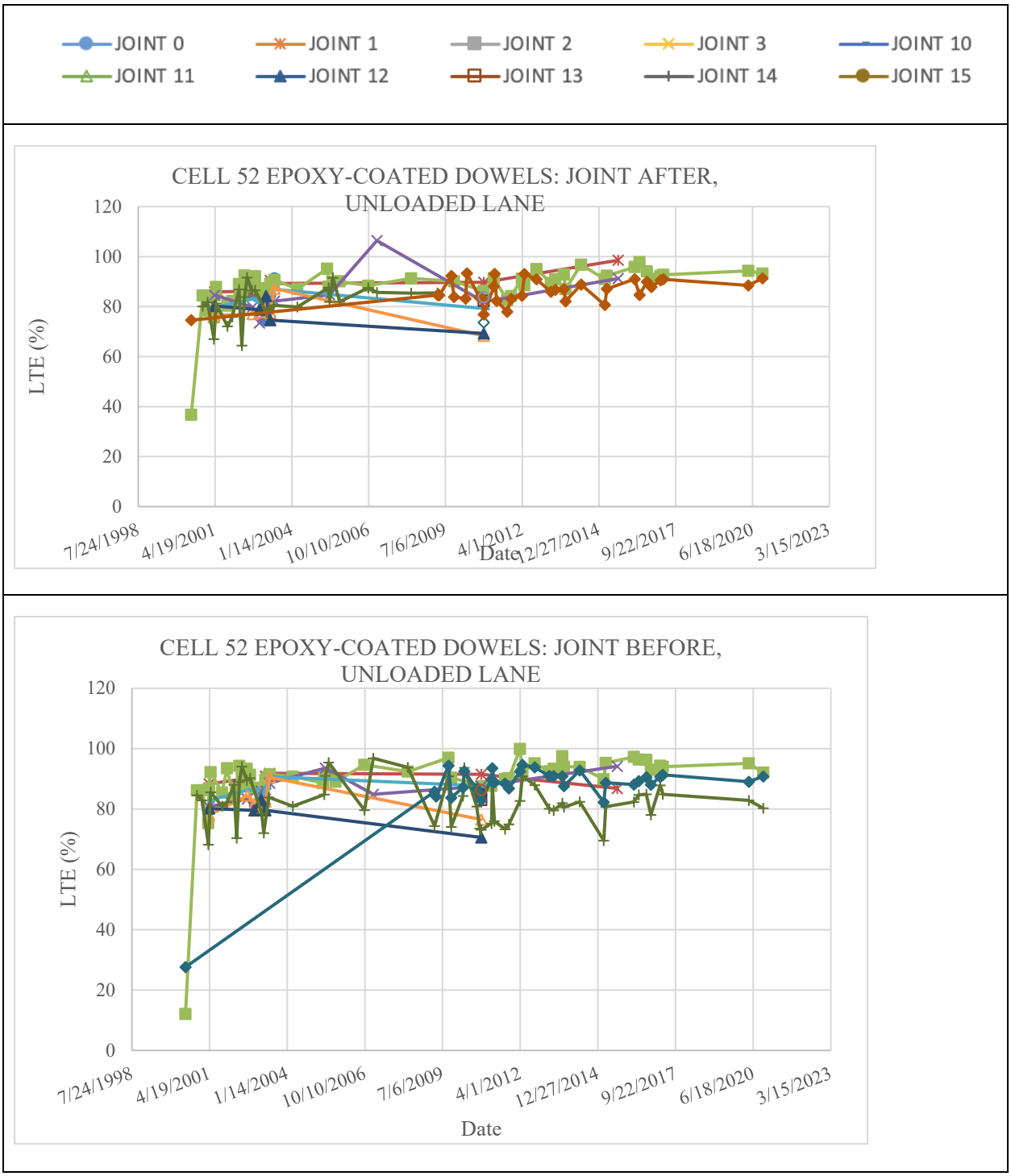

(b)

Figure 3.6 a + b: Cell 52 (epoxy-coated dowels) unloaded lane LTE by joint

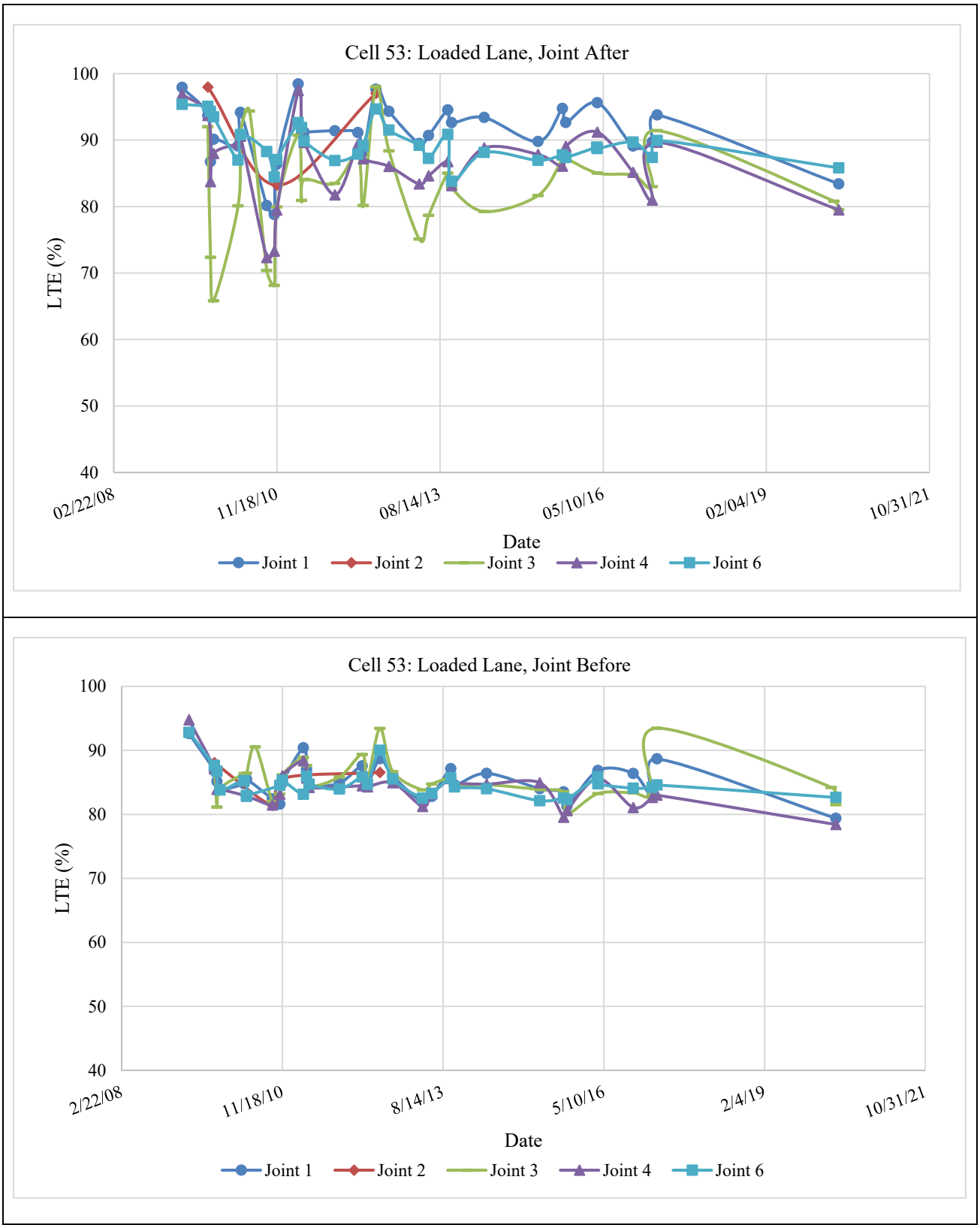
Cell 53: Loaded Lane, Joint After
LTE (%)
100
90
80
70
60
50
40
02/22/08
11/18/10
08/14/13
05/10/16
02/04/19
10/31/21
Date
Joint 1
Joint 2
Joint 3
Joint 4
Joint 6
Cell 53: Loaded Lane, Joint Before
LTE (%)
100
90
80
70
60
50
40
2/22/08
11/18/10
8/14/13
5/10/16
2/4/19
10/31/21
Date
Joint 1
Joint 2
Joint 3
Joint 4
Joint 6

(a)

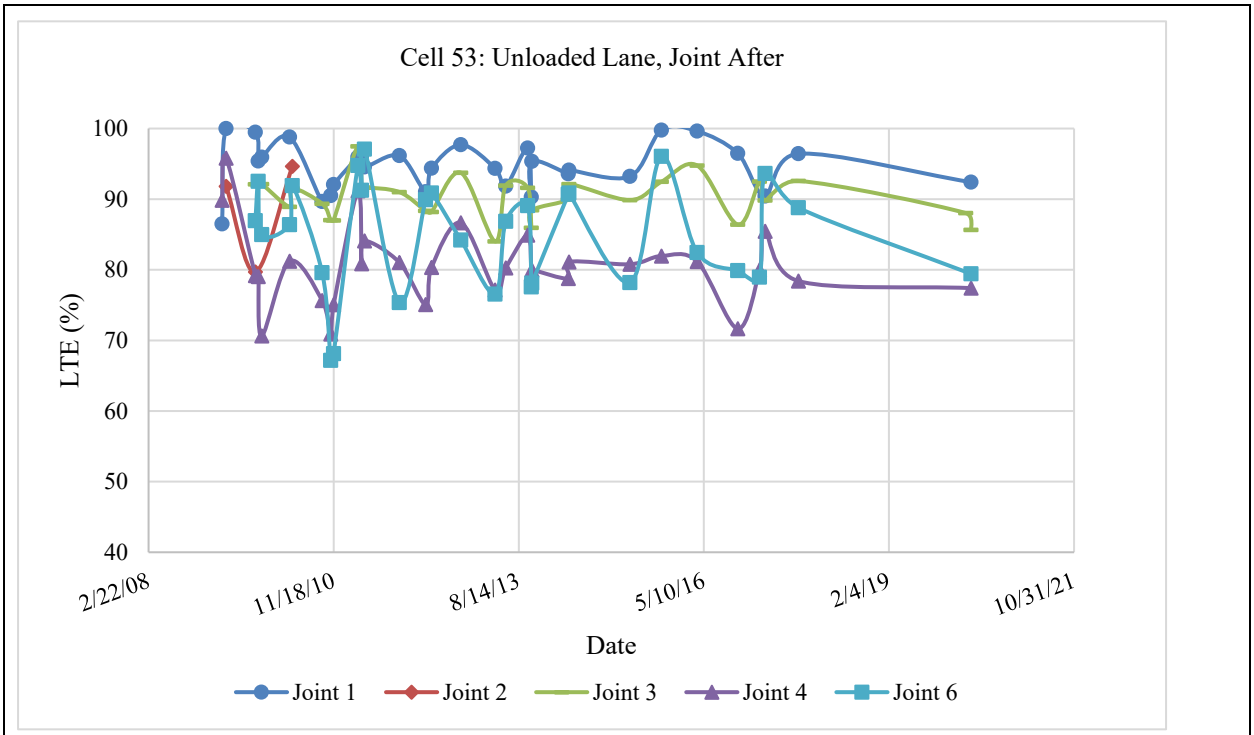

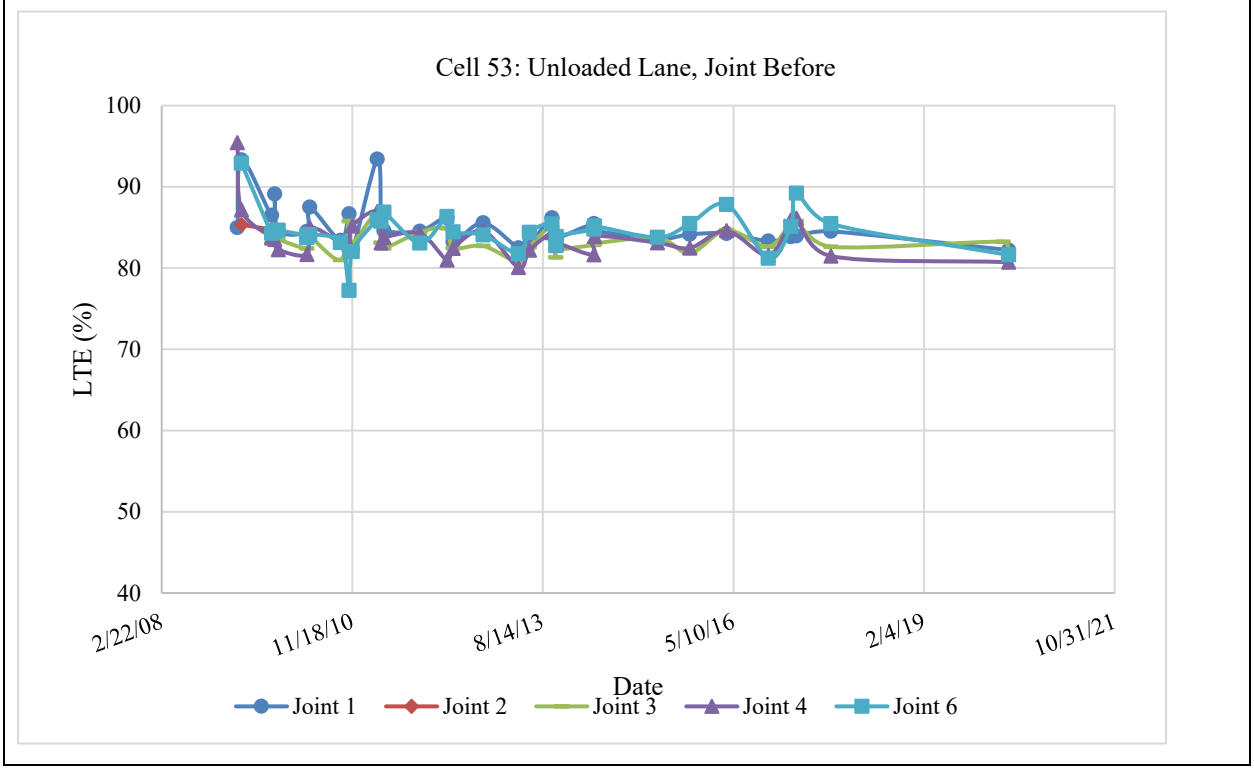

(b)

Figure 3.7 a + b: Cell 53 loaded lane LTE by joint

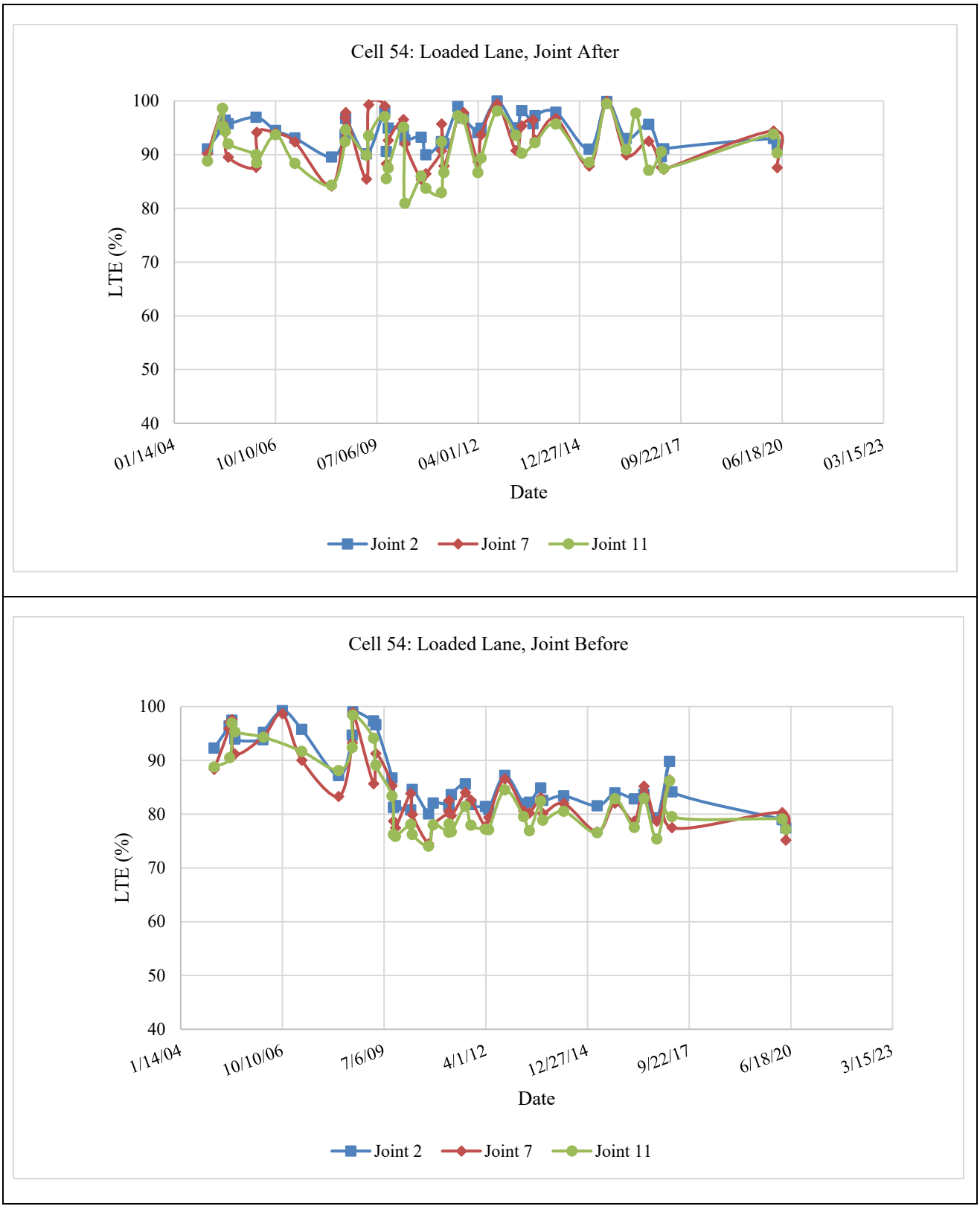
Cell 54: Loaded Lane, Joint After
LTE (%)
100
90
80
70
60
50
40
01/14/04
10/10/06
07/06/09
04/01/12
12/27/14
09/22/17
06/18/20
03/15/23
Date
Joint 2
Joint 7
Joint 11
Cell 54: Loaded Lane, Joint Before
LTE (%)
100
90
80
70
60
50
40
1/14/04
10/10/06
7/6/09
4/1/12
12/27/14
9/22/17
6/18/20
3/15/23
Date
Joint 2
Joint 7
Joint 11

(a)

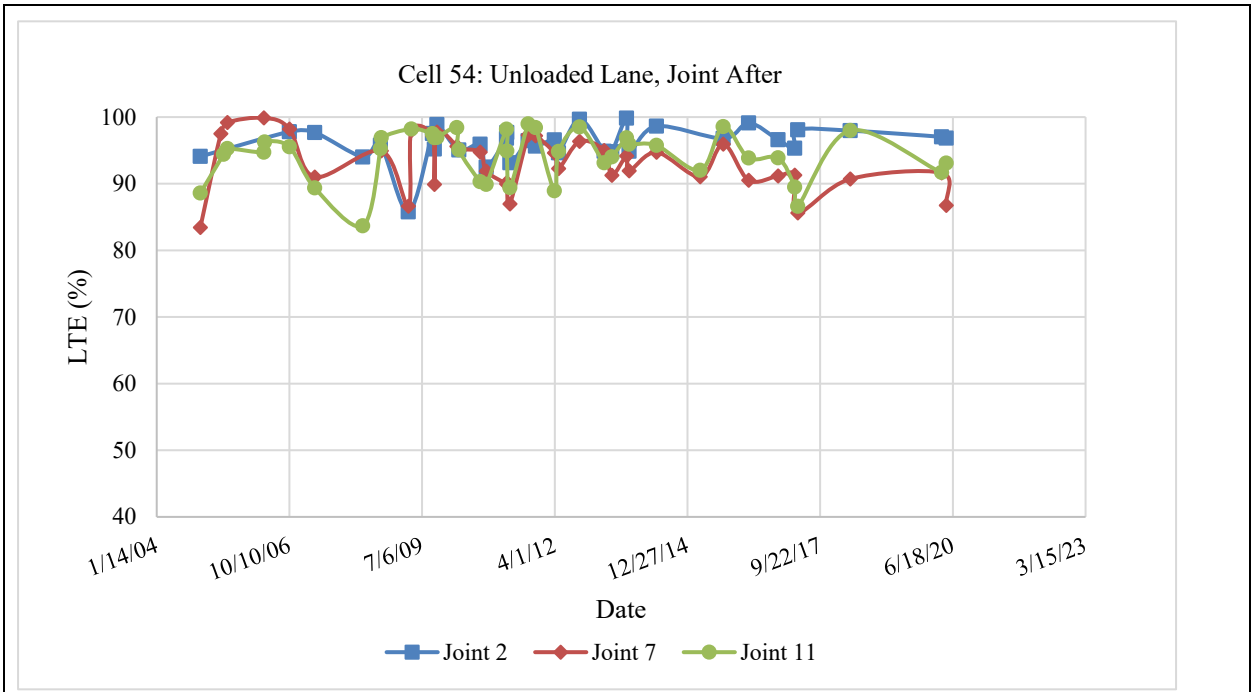

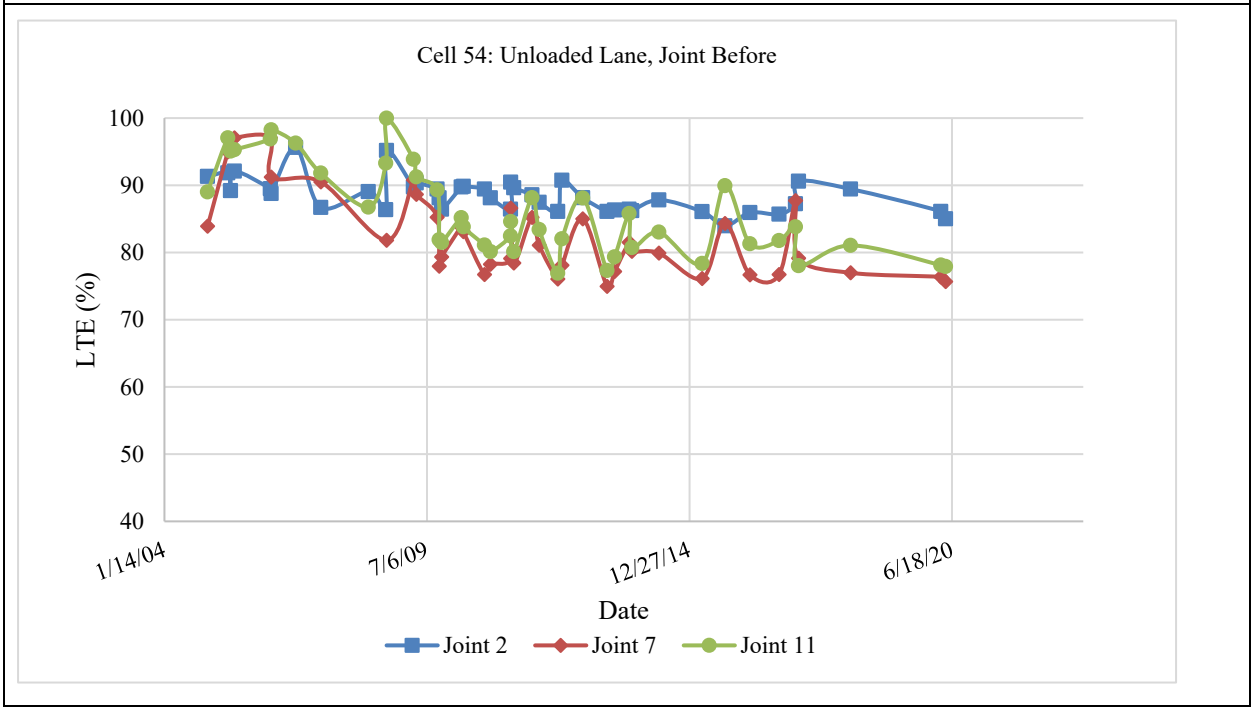

(b)

Figure 3.8 a + b: Cell 54 unloaded lane LTE by joint

The LTE data follows the time series format because each data point is indexed in time order, by Spring versus Fall of each year, meaning the data can be fit to a time-series model. The joint data shows much of the variability that would be expected from time series data, which indicates that an ARIMA model should be used. Using the theory developed in Equations 2 and 3, the best model was fitted to the data and plotted to obtain an equation for predicting LTE for each cell.

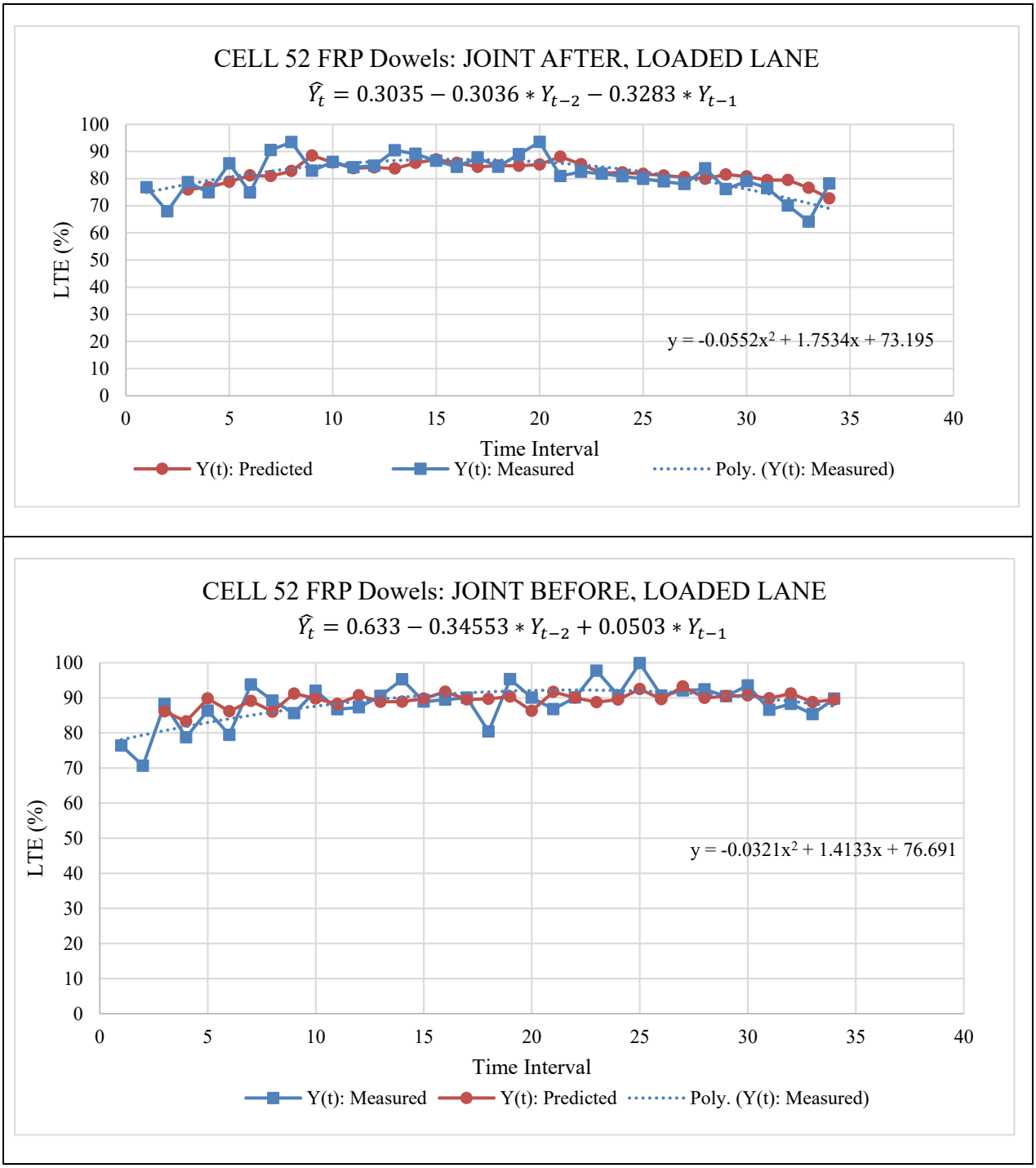
CELL 52 FRP Dowels: JOINT AFTER, LOADED LANE
$\hat{Y}_t = 0.3035 - 0.3036 * Y_{t-2} - 0.3283 * Y_{t-1}$
LTE (%)
Time Interval
y = -0.0552x² + 1.7534x + 73.195
Y(t): Predicted
Y(t): Measured
Poly. (Y(t): Measured)
CELL 52 FRP Dowels: JOINT BEFORE, LOADED LANE
$\hat{Y}_t = 0.633 - 0.34553 * Y_{t-2} + 0.0503 * Y_{t-1}$
LTE (%)
Time Interval
y = -0.0321x² + 1.4133x + 76.691
Y(t): Measured
Y(t): Predicted
Poly. (Y(t): Measured)

(a)

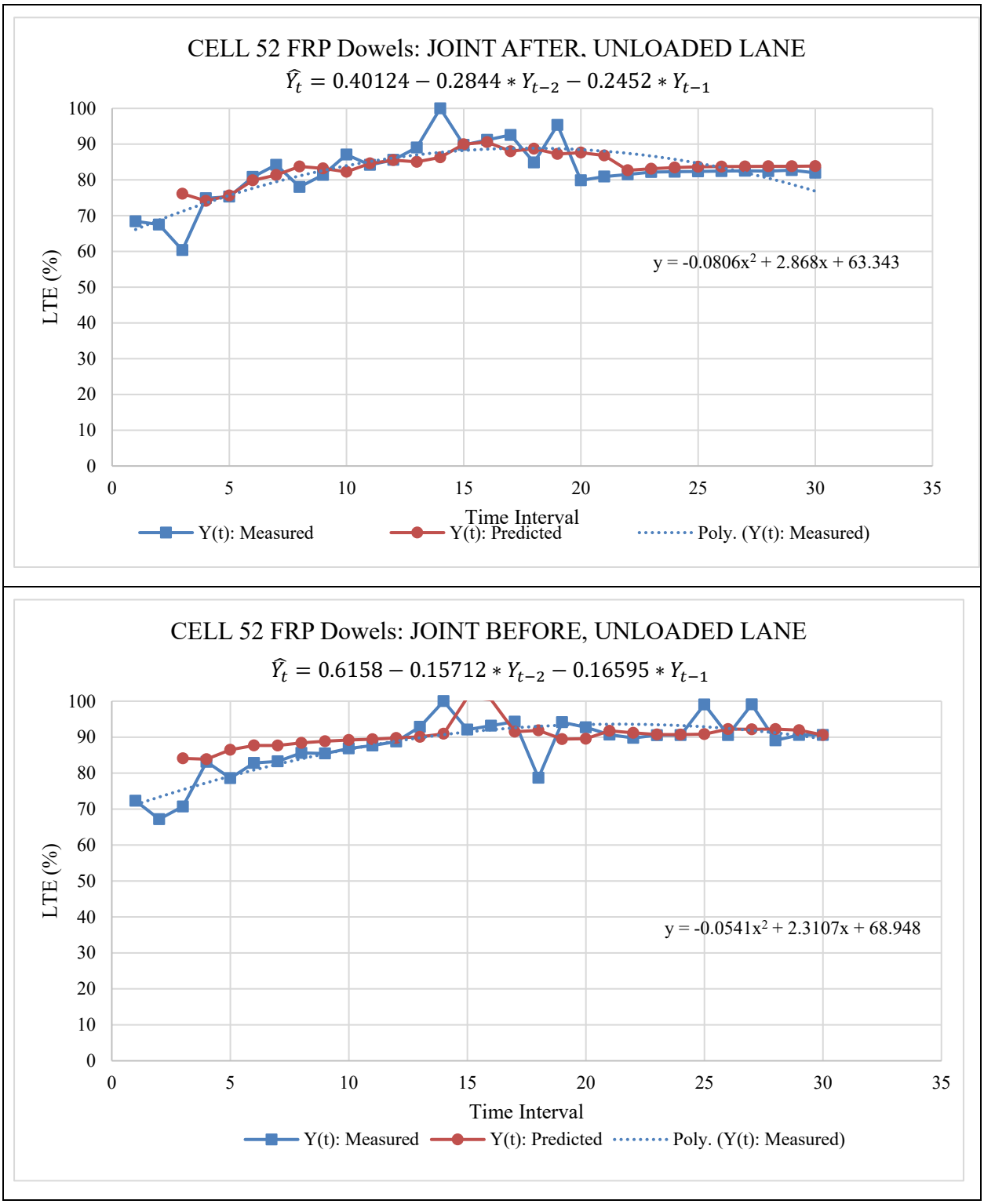

(b)

Figure 3.9 a + b: Time series predictions of Cell 52 loaded lane (FRP dowel bars)

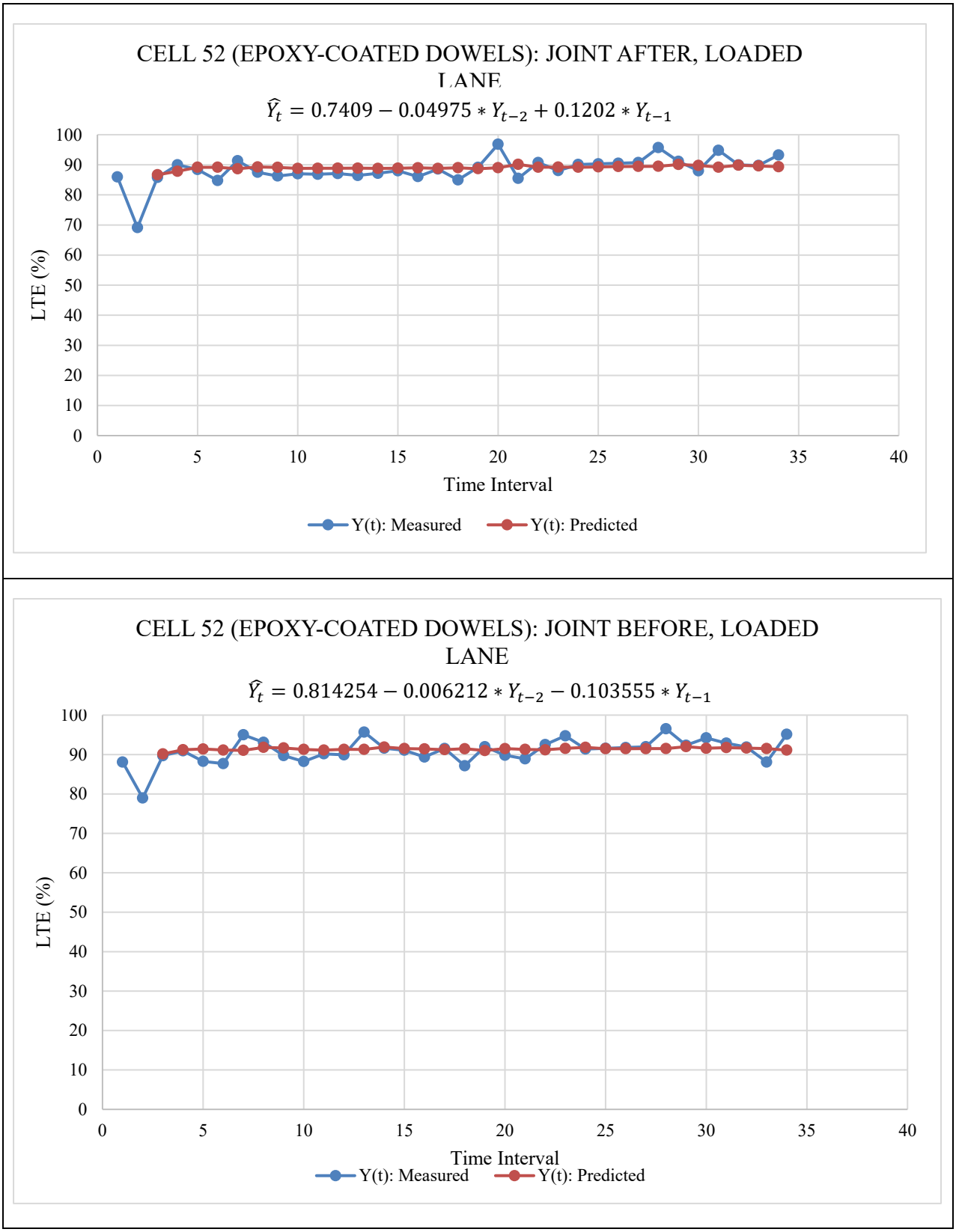
CELL 52 (EPOXY-COATED DOWELS): JOINT AFTER, LOADED LANE
$\hat{Y}_t = 0.7409 - 0.04975 * Y_{t-2} + 0.1202 * Y_{t-1}$
LTE (%)
Time Interval
Y(t): Measured
Y(t): Predicted
CELL 52 (EPOXY-COATED DOWELS): JOINT BEFORE, LOADED LANE
$\hat{Y}_t = 0.814254 - 0.006212 * Y_{t-2} - 0.103555 * Y_{t-1}$
LTE (%)
Time Interval
Y(t): Measured
Y(t): Predicted

(a)

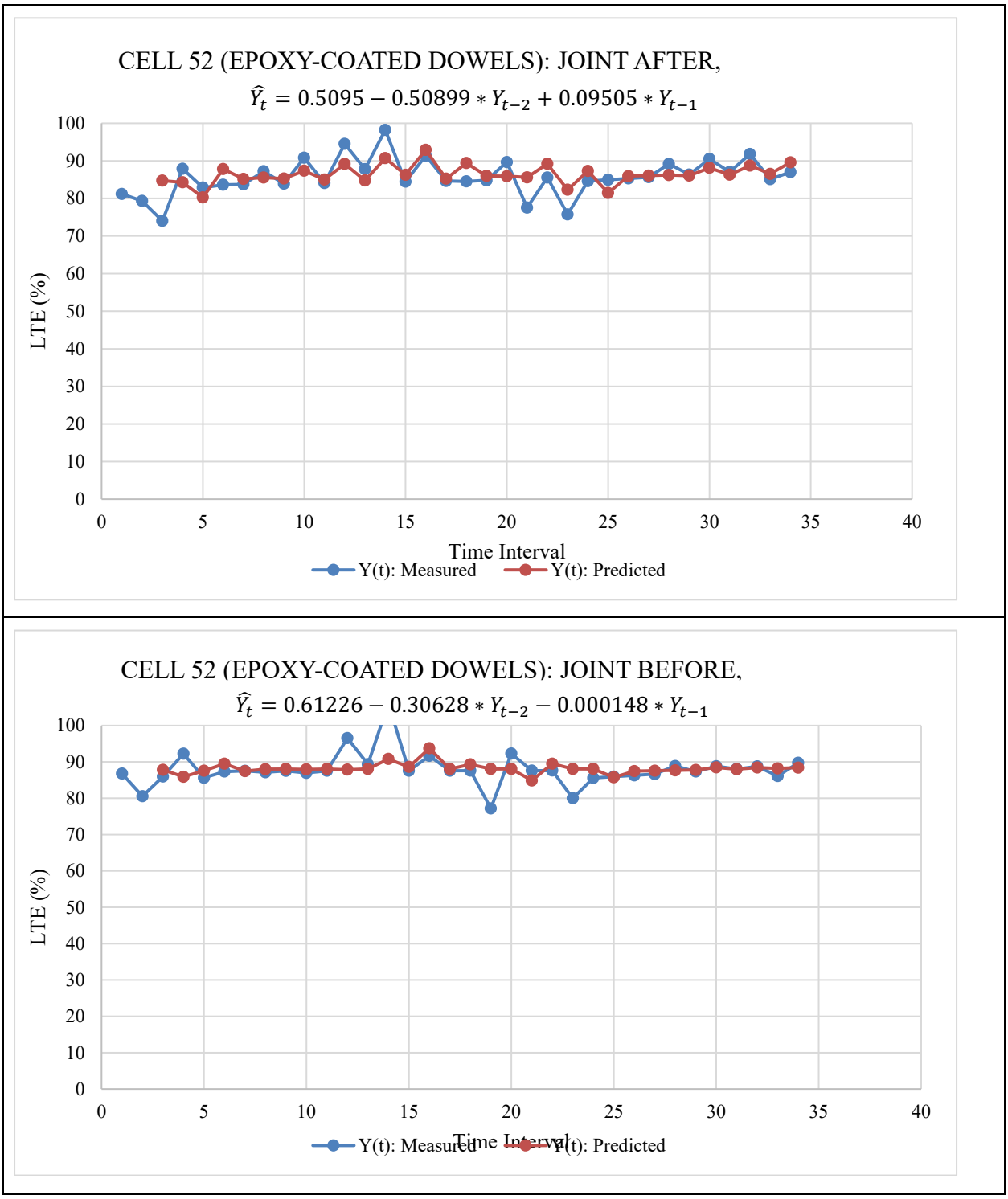

(b)

Figure 3.10 a + b: Time series predictions of Cell 52 loaded lane (epoxy-coated dowel bars)

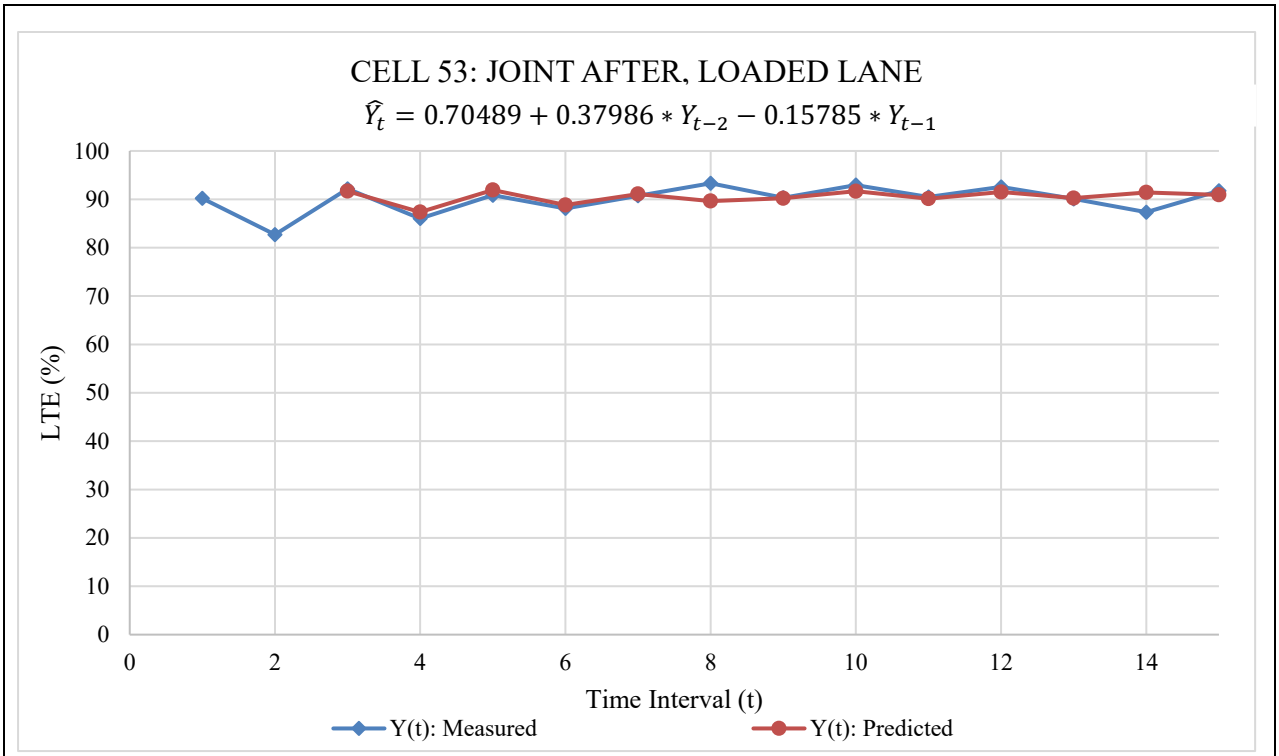
CELL 53: JOINT AFTER, LOADED LANE
$\hat{Y}_t = 0.70489 + 0.37986 * Y_{t-2} - 0.15785 * Y_{t-1}$
LTE (%)
Time Interval (t)
Y(t): Measured
Y(t): Predicted

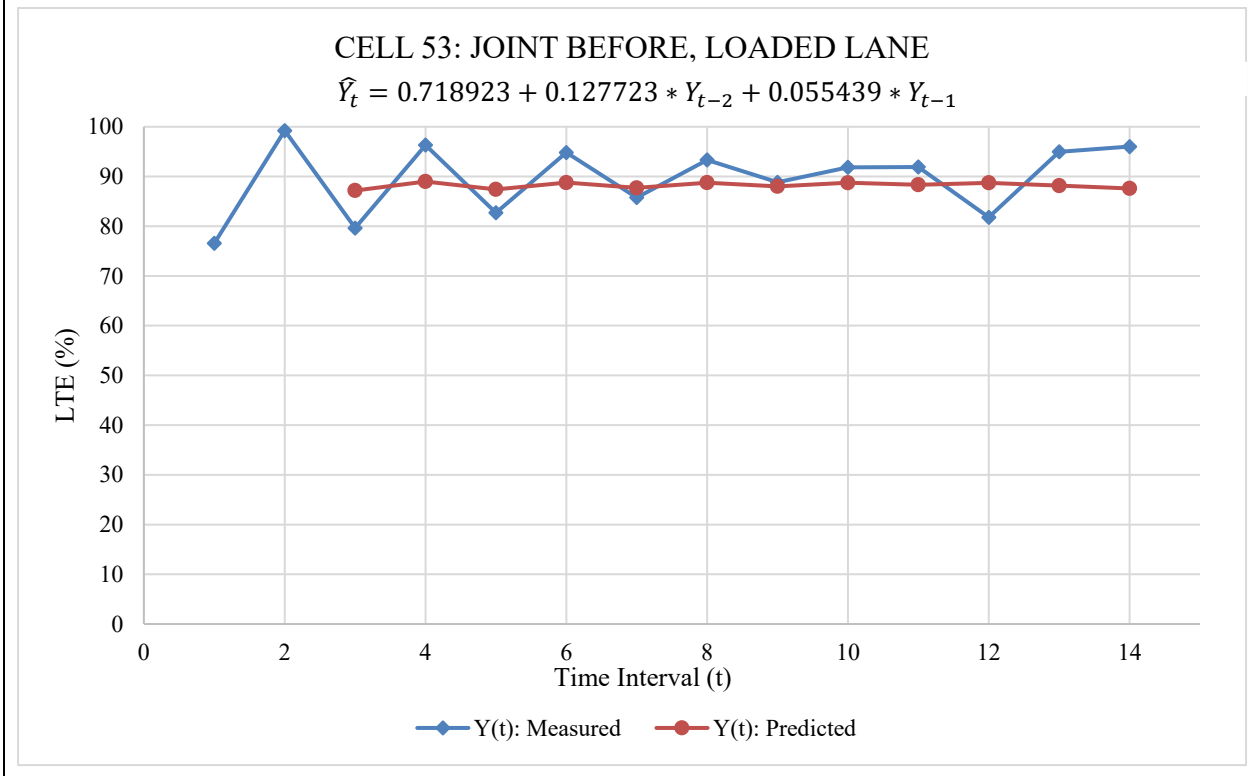
CELL 53: JOINT BEFORE, LOADED LANE
$\hat{Y}_t = 0.718923 + 0.127723 * Y_{t-2} + 0.055439 * Y_{t-1}$
LTE (%)
Time Interval (t)
Y(t): Measured
Y(t): Predicted

(a)

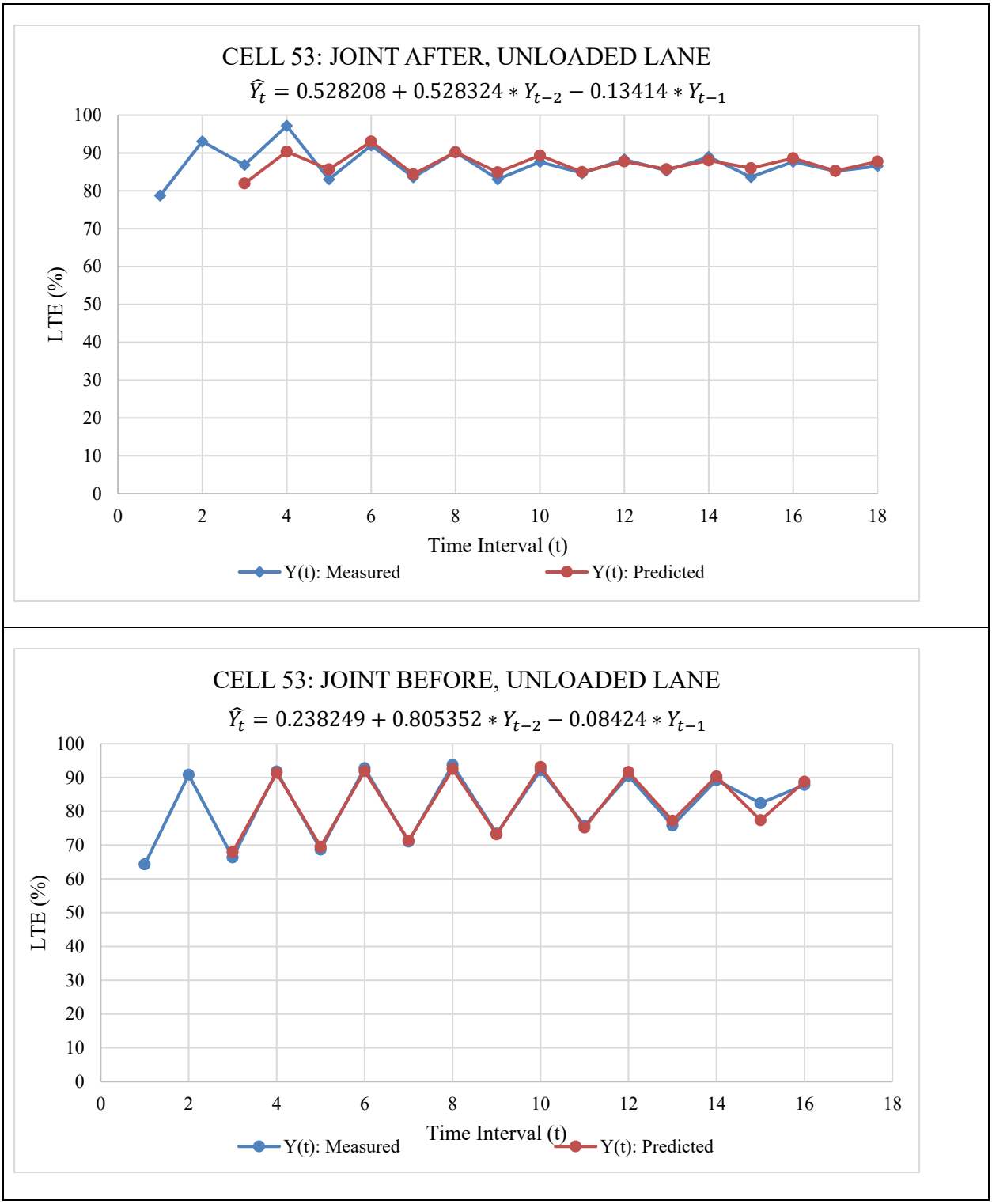

(b)

Figure 3.11 a + b: Time series predictions of Cell 53 (epoxy-coated dowel bars) loaded lane

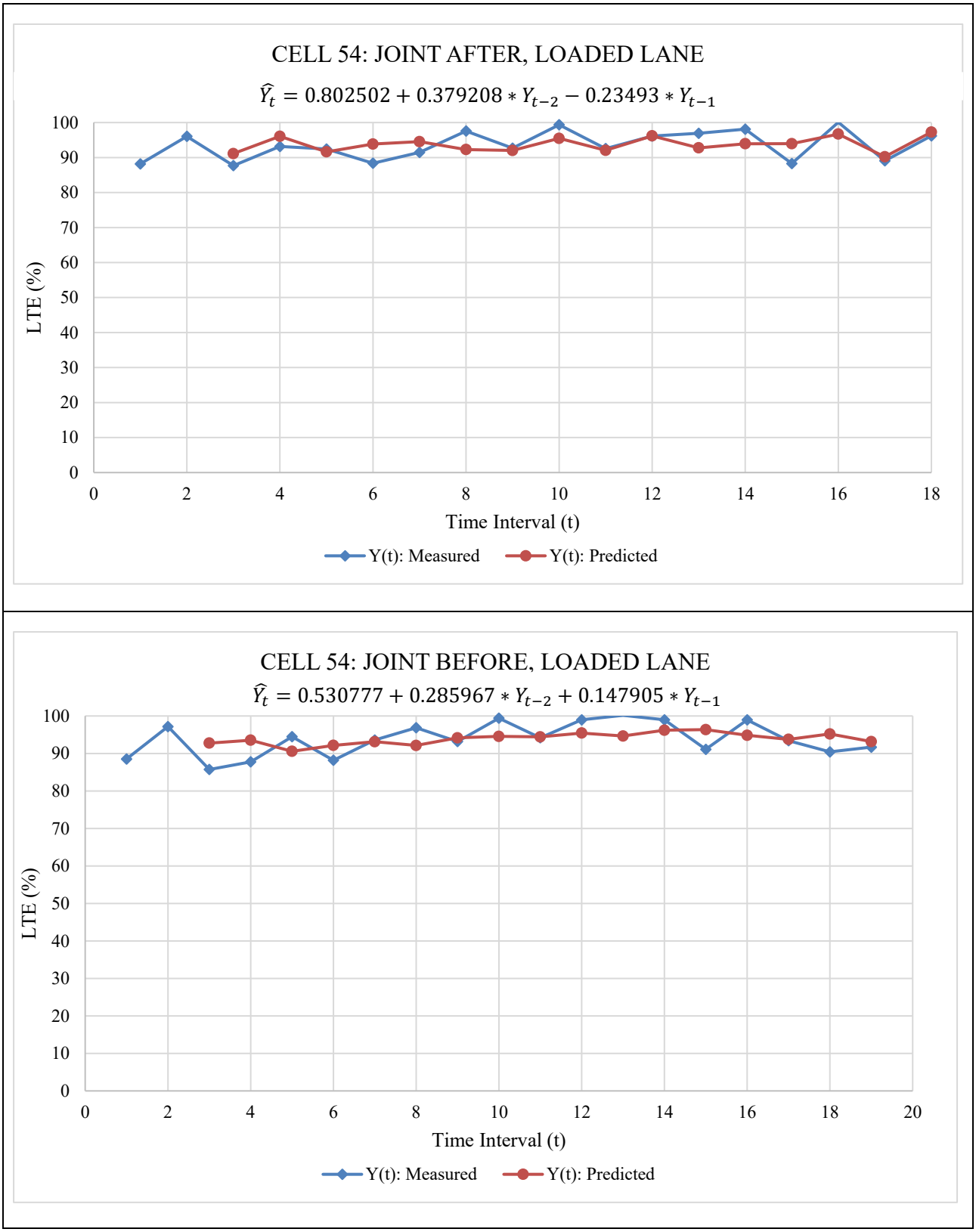
CELL 54: JOINT AFTER, LOADED LANE
$\widehat{Y}_t = 0.802502 + 0.379208 * Y_{t-2} - 0.23493 * Y_{t-1}$
LTE (%)
Time Interval (t)
Y(t): Measured
Y(t): Predicted
CELL 54: JOINT BEFORE, LOADED LANE
$\widehat{Y}_t = 0.530777 + 0.285967 * Y_{t-2} + 0.147905 * Y_{t-1}$
LTE (%)
Time Interval (t)
Y(t): Measured
Y(t): Predicted

(a)

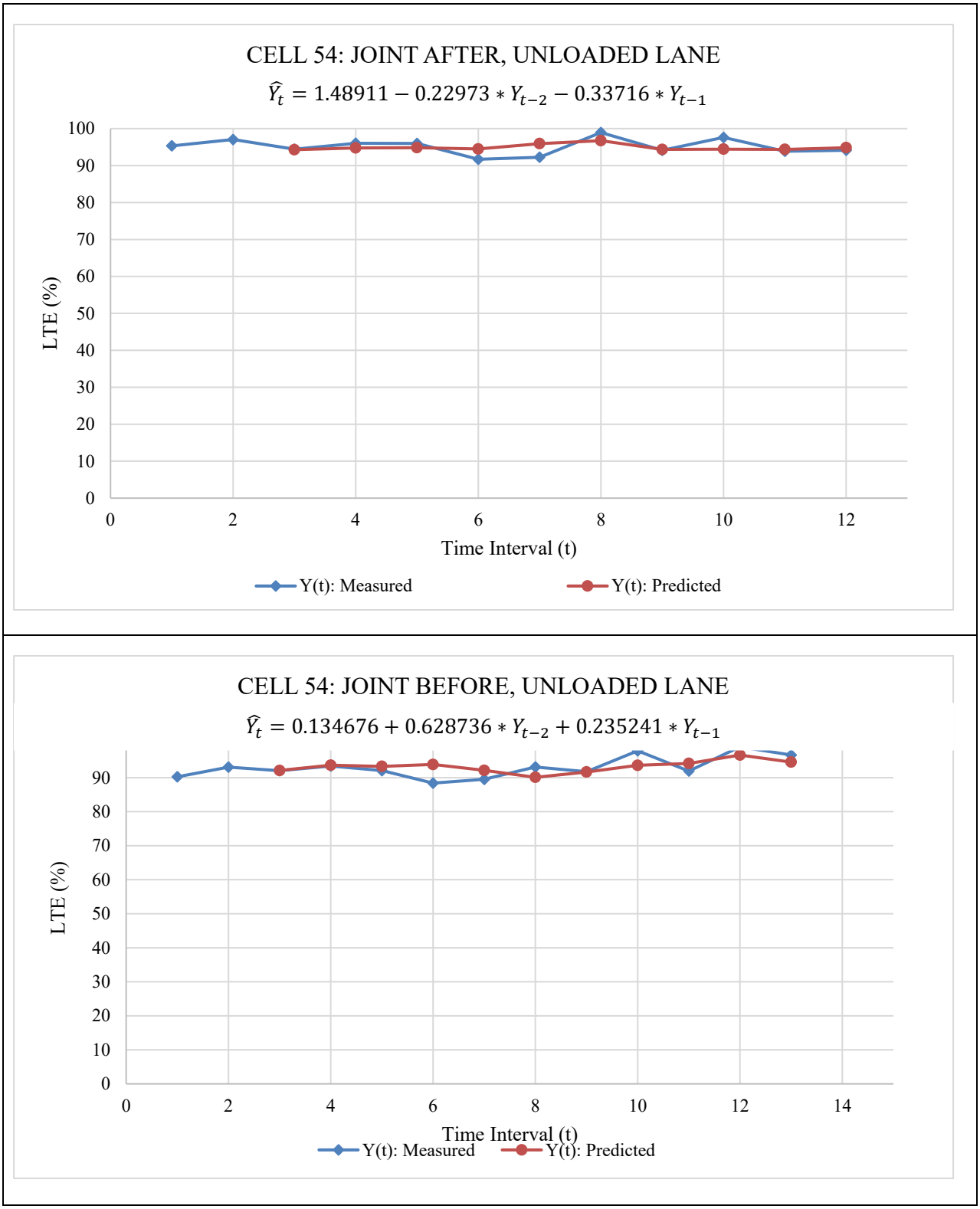

(b)

Figure 3.12 a + b: Time series predictions of Cell 54 (steel dowel bars) loaded lane

Table 3.1: 15 and 30-year predictions for the LTE of FRP, epoxy-coated dowel, and stainless-steel dowel bars.

Cell		15-year Prediction/Data	15-year Average by Lane	30-year Prediction	30-year Average by Lane
52 (FRP dowel bars)	Joint After, Loaded Lane	0.77	0.81	0.83	0.84
	Joint Before, Loaded Lane	0.87		0.85	
	Joint After, Unloaded Lane	0.83	0.87	0.84	0.87
	Joint Before, Unloaded Lane	0.91		0.90	
52 (EPOXY-coated dowel bars)	Joint After, Loaded Lane	0.95	0.94	0.89	0.90
	Joint Before, Loaded Lane	0.93		0.91	
	Joint After, Unloaded Lane	0.87	0.88	0.87	0.88
	Joint Before, Unloaded Lane	0.88		0.88	
53 (stainless-steel dowel bars)	Joint After, Loaded Lane	0.91	0.89	0.91	0.89
	Joint Before, Loaded Lane	0.88		0.88	
	Joint After, Unloaded Lane	0.87	0.86	0.87	0.86
	Joint Before, Unloaded Lane	0.86		0.85	
54 (epoxy-coated dowel bars)	Joint After, Loaded Lane	0.94	0.94	0.94	0.94
	Joint Before, Loaded Lane	0.94		0.94	
	Joint After, Unloaded Lane	0.95	0.97	0.95	0.97
	Joint Before, Unloaded Lane	0.98		0.99	

CHAPTER 4: DISCUSSION

4.1 ANALYSIS BY STRESS AND LOAD LEVEL

4.1.1 Cell 52 FRP Dowel Bars

Beginning with the joints of cell 52 which correspond to the FRP dowel bars, Figure 3.1 shows a significant amount of data for drawing conclusions for stresses of 365 kPa and 550 kPa, but less for 730 kPa. All LTEs are near 0.8. Figure 3.3, showing Cell 52 organized by joint, indicates much more data variability between the different joints in the measurements after the joint. The measurements before the joint seem to be tightly clustered together by joint, and there is an initial decrease in LTE before it levels out approximately at 0.8. The measurements after the joint are not clustered tightly, making it difficult to determine an average LTE.

4.1.2 Cell 52 Epoxy-Coated Dowel Bars

Beginning with the joints of cell 52 which correspond to the FRP dowel bars, Figure 3.4, showing Cell 52 organized by joint, indicates much more data variability between the different joints in the measurements after the joint. The measurements before the joint seem to be tightly clustered together by joint, and there is an initial decrease in LTE before it levels out approximately at 0.9. The measurements after the joint are not clustered tightly, making it difficult to determine an average LTE. The overall data seems to show that the data from the joints corresponding to the epoxy-coated dowel bars have a higher LTE compared to those corresponding to the FRP dowel bars.

4.1.3 Cell 53

Cell 53 shows similar trends to Cell 52. Figure 3.2 also has more data points for the lower stresses (365 kPa and 550 kPa) and the LTEs are approximately 0.85. Figure 3.5 shows more data variability in measurements after the joint, and more tightly clustered data in the measurements before the joint. The LTEs observed in Cell 53 are slightly higher than the LTEs of the joints with FRP dowels in Cell 52, pointing to the efficiency of the fiber reinforced plastic dowels. However, the substantial difference between the slab thickness and support layers of Cells 52 and 53 may also contribute to these similarities. Table 3.1 confirms this, as the average 15- and 30-year predictions for Cells 52 and 53 are very similar. Cell 52 has the higher 15-year prediction, but Cell 53 has the higher 30-year prediction.

4.1.4 Cell 54

As seen in Figure 3.2, the inside lanes and outside lanes follow the same trends, regardless of whether the LTE measurement was taken before or after the joint. The LTEs measured before the joint are slightly lower than the LTEs after the joint. In Figure 3.6, Cell 54 shows greater data variability in the measurements before the joint, unlike Cell 52 and 53. However, it does show a similar initial decrease in LTE as Cell 52, and a similar flatline of data around an LTE of 0.8. The measurements after the joint all show an LTE of around 0.85. As seen in Figure 1.1, Cells 54 and 52 have similar slab thicknesses so the

comparison between them should be mostly due to differences in the dowel bars, although the different base layers of the two cells are quite different and should be noted.

All the cells are seen to have high and effective LTEs in the dataset that is plotted. The majority of the data points from the past 15 years all point to average LTEs around 0.8 or 0.85. The cells all show sufficiently high LTEs, and the trends in the data and statistical predictions seem to show a trend towards a constant value of LTE. That being said, it is impossible to predict the future and degradation of concrete joints due to loads and environmental effects causing a decrease in LTE is likely.

4.2 TIME SERIES MODELING

The time series models were obtained by choosing the load level which gave the largest amount of data, clustered in Fall and Spring of every year so the models are accurate and minimize the amount of interpolation (linear or polynomial). The models given in Figures 3.7-3.10 for Cells 52-54 fit the data well, with small sums of squared errors, as this was minimized by Excel's solver. The data was tested for stationarity, and most of the data was deemed stationary, meaning that the mean is presumed constant and there are no moving average (MA) terms in the equations.

From the data analysis by joint, it was expected that Cell 52 would have the most variability in its time series data, which was confirmed by the predicted time series model have the most inconsistency. Cell 54 had the least amount of variability in the model, as it predicts a near constant line for most of the subsets of the data. The model for Cell 53 falls between those of Cells 52 and 54. As seen in Figure 3.7, the time series data has a significant amount of fluctuation, although fitting the data to an order 2 polynomial shows that the overall trend is decreasing and the leading coefficients in the fitted polynomials are all negative. It is similar for cells 53 and 54.

The time series predictions seem to be overestimating the LTE, as the slabs show a plateauing of LTE between 80-85% and most of the predictions are above 85%. Table 3.1 indicates that Cells 52 and 53 have similar LTEs over time, averaging between 81-89% at the 15-year prediction, but Cell 53 has the slightly higher estimates. In contrast, Cell 54 has a much higher predicted LTE of greater than 94%, which is unlikely because the data had a slightly decreasing trend in previous years, and it is unusual that the LTE would increase over time. This error could possibly be due to the interpolation of data in the model development, as well as the way the model data was chosen from the overall dataset. For a more accurate model, choosing different stress levels may give a larger dataset, and doing the model development process by joint in each cell would give a model which reflects the behavior of the individual joints would be useful in seeing if there are trends based on the dowel bar type in each joint.

The conclusion that can be drawn is that Cells 52-54 all seem to maintain a high LTE over time which seems to be nearly constant. Similarly, for the 30-year predictions, Cells 52 and 53 have averages of 0.84, 0.87 and 0.89, 0.86 respectively, whereas Cell 54 has predictions of 0.94 and 0.97, remaining constant from the 15-year predictions.

Therefore, it seems that there are only small differences between the performances of the cells themselves, indicating highly effective designs for all dowel types compared. The designs of the cells have significant differences beyond the dowel bar types, so other factors may contribute to the performance of the sections. Based on the models developed in this research, the fiber reinforced plastic (FRP) dowels seem to be a respectable alternative to the stainless steel and conventional epoxy-coated dowels with respect to the load transfer efficiency.

4.3 RIDE QUALITY (IRI) DATA

The International Roughness Index (IRI) provides a quantification of the ride quality of a surface. It is based on the quarter car dynamics, which captures the effect of vertical acceleration of the quarter car over a stretch of road and provides a summation of vertical displacements per unit horizontal displacement. In this research, IRI helps to better understand the pavement wholistically and to corroborate the previously discussed conclusions.

The inside (loaded) lane IRI data can be seen in Figure 4.1**,** showing relatively similar IRI over time for Cells 52 and 54 of around 2 m/km. Cell 53 has a higher IRI, centering around 2.25 m/km, all of which are very high IRI values. Major anomalous spikes are explained by construction events and possible construction debris and not by performance. Minor fluctuations are attributed to seasonality.

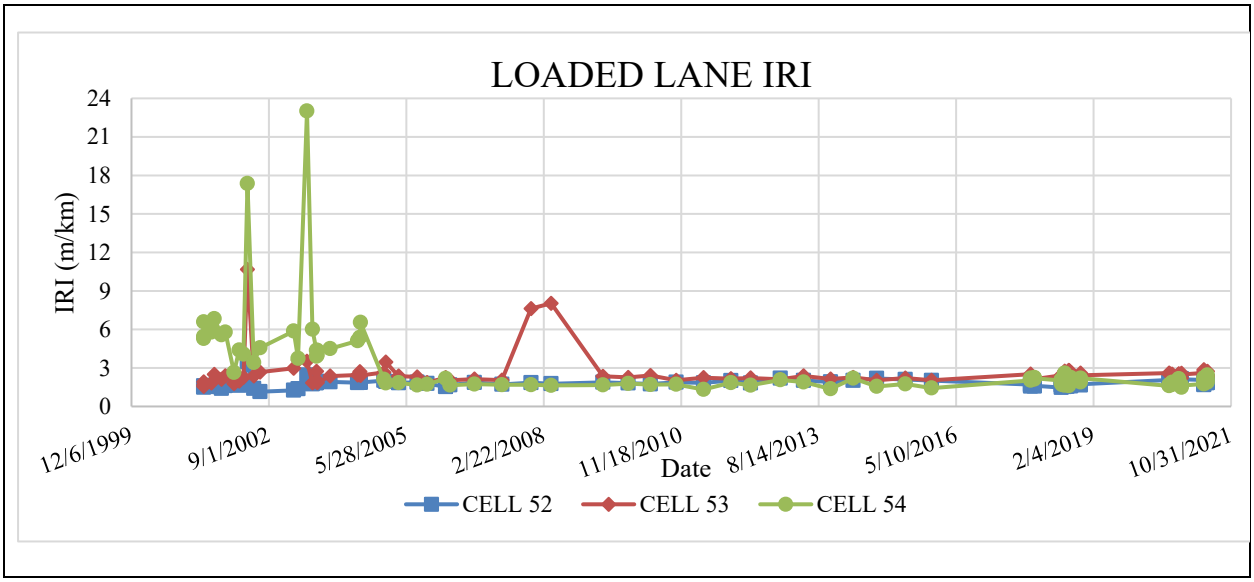

Figure 4.1: Cells 52, 53, and 54 inside lane IRI over time

The outside (unloaded) lane IRI data is represented in Figure 4.2, with Cell 52 having the highest IRI near 2.5 m/km, Cell 53 and 54 near 2 m/km. Since the outside lane has no traffic, it acts as an environmental control. The IRI of Cell 52 is similar to the other cells in both the inside and outside lanes, and there is no significant decrease in IRI for any of the cells over time. As in Figure 4.1, anomalous spikes in IRI are explained by construction events and possible construction debris and not by performance. Minor fluctuations are attributed to seasonality.

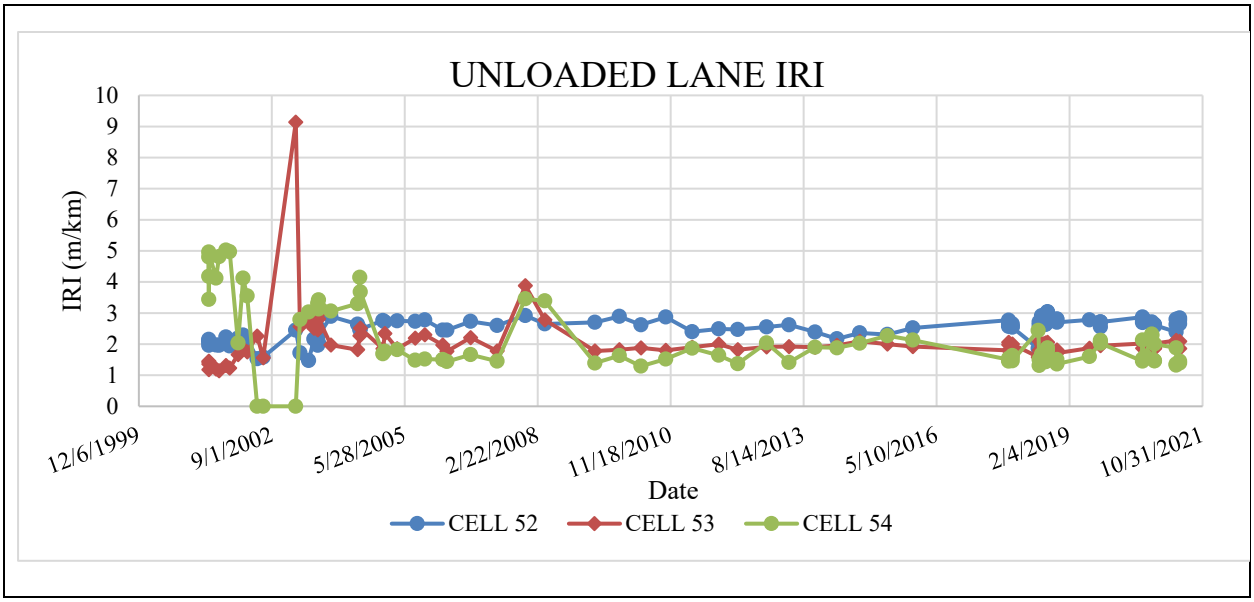

Figure 4.2: Cells 52, 53, and 54 outside lane IRI over time

CHAPTER 5: CONCLUSIONS

Cells 52, 53, and 54 show highly effective LTEs that are consistent with their 15- and 30-year predictions. Based on trends, it can be inferred that the LTEs would continue to be at or above 80% and the pavement would continue to show a sufficient response to dynamic loads for a long time. Averages for the inside lane (where load is applied at MnROAD) for the 15-year predictions for the FRP dowels are higher than those for the stainless-steel dowels, and similar to those for the epoxy-coated dowels. The 30-year predictions stay the same for the stainless-steel dowels and the epoxy-coated dowels but decrease slightly for the FRP dowels. Even with this slight decrease in LTE over the latter half of 30 years post-construction, the FRP dowels still show good performance quality compared to the stainless steel and epoxy-coated dowels. The IRI data further validates the conclusions drawn from the LTE analysis, with no unexpected differences in ride quality between the cells over time. Future use of the fiber reinforced plastic dowels should be dependent on time and intensity of construction, available materials, and other external factors. FRP dowels are lighter and easier to install than traditional epoxy-coated dowels and stainless-steel dowels. Based on their performance observed through FWD testing, fiber reinforced plastic dowels have a comparable response to different dynamic loads as other previously used dowels at the current time. According to the models developed in this paper, the fiber reinforced plastic dowel bars should provide an effective response to different dynamic loads for PCC concrete pavements throughout a 30-year lifetime.

Whereas pavement structures were not normalized, LTE is a function of the mechanical load transfer aggregate interlock and the base. Cell 52 was a thinner concrete design than cells 53 and 54, so this corroborates the comparable performance of the FRP dowel bars.

CHAPTER 6: REFERENCES

1. Minnesota Department of Transportation. (2021). *MnROAD*. Retrieved from http://www.dot.state.mn.us/mnroad/
2. Burnham, T. R. (2001). *Construction Report for MnROAD PCC Test Cells 32, 52, and 53.* (No. MN/RC 2002-04). St. Paul, MN: Minnesota Department of Transportation.
3. Federal Highway Administration. (2021). *FHWA (Federal Highway Administration) LTPP (Long-Term Pavement Performance) InfoPave.* Retrieved from https://InfoPave.fhwa.dot.gov/?Goto=Home
4. Izevbekhai, B. I., & Ubani, B. N. (2015). *Seven-Year Performance Report on MnROAD High Performance Concrete Design Test Cell 53* (No. MN/RC 2015-38). St. Paul, MN: Minnesota Department of Transportation.
5. Izevbekhai, B. I., & Rohne, R. J. (2008). MnROAD Cell 54: Cell Constructed with Mesabi-Select (Taconite-Overburden) Aggregate; Construction and Early Performance (No. MN/RC 2008-18). St. Paul, MN: Minnesota Department of Transportation.
6. Larson, R. M., & Smith, K. D. (2011). *Evaluation of Alternative Dowel Bar Materials and Coatings.* Columbus, OH: Ohio Department of Transportation Office of Research and Development.
7. Minnesota Department of Transportation. (2021). *MnROAD FWD (Falling Weight Deflectometer) Testing Guide.* Retrieved from http://www.dot.state.mn.us/mnroad/files/mnroad-fwd-final-2014.pdf
8. PennState Department of Statistics. (2021). *STAT 510 Applied Time Series Analysis.* Retrieved from https://online.stat.psu.edu/stat510/
9. Hyndman, R. J., & Athanasopoulos, G. (2018). *Forecasting: Principles and Practice*. University of Crawley WA 6009, Australia OTexts. Retrieved from https://robjhyndman.com/uwafiles/fpp-notes.pdf 12/3/22.
10. Izevbekhai, B. I. (2016). Pavement Surface Characteristics Concrete New Construction (MnRoad Study) (No. MN/RC 2015-48). St. Paul, MN: MnDOT.
11. Kuha, J. (2004). AIC and BIC: Comparisons of Assumptions and Performance. *Sociological Methods & Research*, *33*(2), 188–229.
12. Gavin, H. P. (2019). *The Levenberg-Marquardt Algorithm for Nonlinear Least Squares Curve-Fitting Problems*. Department of Civil and Environmental Engineering, Duke University. Durham NC USA
13. Sayers, M. W. (1995). On the Calculation of International Roughness Index from Longitudinal Road Profile. *Transportation Research Record, 1501*, Washington DC USA